

Copyright
by
Shiri Avnery
2007

**1,400 Years of Biomass Burning, Climate Variability, and
Environmental Change on Ometepe Island, Lake Nicaragua**

by

Shiri Avnery, B.S.

Thesis

Presented to the Faculty of the Graduate School of

The University of Texas at Austin

in Partial Fulfillment

of the Requirements

for the Degree of

Master of Arts

The University of Texas at Austin

May 2007

**1,400 Years of Biomass Burning, Climate Variability, and
Environmental Change on Ometepe Island, Lake Nicaragua**

**Approved by
Supervising Committee:**

Supervisor: Robert Dull

Kelley Crews-Meyer

Timothy Keitt

Acknowledgements

I would like to thank my advisor, Dr. Robert Dull, for all of his help and patience throughout the data compilation and writing stages of this project. I am extremely grateful to Dr. Timothy Keitt for teaching me the primary mode of analysis employed in this thesis, as well as to Dr. Kelley Crews-Meyer for all of her insightful comments and personal support over the past two years. Finally, I would like to thank all of the faculty and staff of the Department of Geography and the Environment for making my experience at the University of Texas - Austin incredibly edifying and enjoyable.

May 4th, 2007

Abstract

1,400 Years of Biomass Burning, Climate Variability, and Environmental Change on Ometepe Island, Lake Nicaragua

Shiri Avnery, M.A.

The University of Texas at Austin, 2007

Supervisor: Robert Dull

This study examines the relationship between short-term climate variability, paleo-fires, and anthropogenic sources of environmental change over the past 1,400 years on Ometepe Island, located in the tropical dry forests of southwestern Nicaragua. Macroscopic charcoal, loss on ignition, and magnetic susceptibility records were reconstructed from a lake sediment core, and statistical wavelet analyses were performed to contextualize natural fire regimes in this under-investigated tropical biome. Results from this project suggest that fire regimes on Ometepe Island respond to high frequency (sub-centennial scale) climate variations potentially due to the 11- and 22-year sunspot cycles and/or the El Niño Southern Oscillation, with dominant periodicities of ~7, 14, and 24 years. Results additionally support regional paleoenvironmental analyses by providing evidence of anthropogenic environmental impacts between ~600 and 1500 A.D. with a drastic decline after European contact, as well as evidence of widespread drought conditions between 800 - 1000 A.D. and 1150 – 1300 A.D.

Table of Contents

List of Tables	viii
List of Figures.....	ix
Chapter 1 Introduction.....	1
Overview	1
Environmental Setting	6
Cultural History	8
Roadmap	11
Chapter 2 Literature Review.....	12
1. Paleoclimatology.....	13
2. Paleoecology.....	15
Overview of Paleoproxies	18
Macroscopic Charcoal	18
Loss on Ignition	18
Magnetic Susceptibility	19
3. Wavelet Analysis of Geophysical Data	19
Summary	22
Chapter 3 Methods and Results	23
Methods.....	23
Results.....	27
Time Series Data	27
Wavelet Transform Analysis	29
Charco Verde Wavelet Power Spectra.....	29
Charco Verde Wavelet Coherence.....	30
Comparison to ENSO Reconstructions.....	30
Comparison to Solar Activity Reconstructions	31
Chapter 4 Discussion, Implications, and Conclusions.....	33
Discussion.....	33

Sources of Macroscopic Charcoal Fluctuations	33
Significance of Proxy Record Covariance	34
Summary of Natural versus Anthropogenic Sources of Environmental Change on Ometepe Island	36
Conclusions.....	40
Implications.....	43
Appendix A Wavelet Power Spectra	59
A1 Macroscopic Charcoal.....	59
A2 Loss on Ignition	60
A3 Magnetic Susceptibility.....	61
Appendix B Charco Verde Wavelet Coherency Spectra	62
B1 Macroscopic Charcoal - Loss on Ignition	62
B2 Macroscopic Charcoal - Magnetic Susceptibility	63
B3 Magnetic Susceptibility - Loss on Ignition	64
Appendix C Regional Climate Proxy Wavelet Coherency Spectra.....	65
C1 Macroscopic Charcoal - Quelcayya Snow Accumulation.....	65
C2 Macroscopic Charcoal - SOI Reconstruction.....	66
C3 Macroscopic Charcoal - Northern Hemisphere Radiocarbon ($\Delta^{14}\text{C}$).....	67
C4 Macroscopic Charcoal - Sunspot Reconstruction	68
Appendix D Paleoproxy Data	69
References.....	78
Vita	92

List of Tables

Table 1:	Cultural history of indigenous communities on Ometepe Island from 2000 B.C.	46
Table 2:	Radiocarbon sampling and age calibration results.....	47
Table 3:	Summary of time and scale of wavelet power maxima in proxy records analyzed	47
Table 4:	Summary of time and scale of wavelet coherency maxima of proxy records analyzed.....	48

List of Figures

Figure 1:	Site map depicting Ometepe Island and Laguna Charco Verde within southwestern Nicaragua	49
Figure 2:	Depth-age (calibrated in years A.D.) relationship of the Charco Verde lake sediment core.....	49
Figure 3:	Time series results of the Charco Verde lake sediment core	50
Figure 4:	Wavelet power spectra and time series plots of the Charco Verde paleoproxies	51
Figure 5:	Wavelet coherency plots of the Charco Verde paleoproxies	52
Figure 6:	Wavelet power spectrum and time series plot of Quelcayya ice core snow accumulation.....	53
Figure 7:	Wavelet coherency plots of Quelcayya ice core snow accumulation and Charco Verde proxies	53
Figure 8:	Wavelet power spectrum and time series plot of reconstructed winter Southern Oscillation Index	54
Figure 9:	Wavelet coherency plots of reconstructed winter Southern Oscillation Index and Charco Verde proxies.....	54
Figure 10:	Wavelet power spectrum and time series plot of northern hemisphere radiocarbon ($\Delta^{14}\text{C}$).....	55
Figure 11:	Wavelet coherency plots of northern hemisphere radiocarbon ($\Delta^{14}\text{C}$) and Charco Verde proxies	55
Figure 12:	Wavelet power spectrum and time series plot of group sunspot number (SN).....	56
Figure 13:	Wavelet coherency plots of group sunspot number (SN)	56

Figure 14: Wavelet power spectra of reconstructed winter SOI and Charco Verde proxies over the time period 1706-1977 A.D.57

Figure 15: Wavelet power spectra of group sunspot number and Charco Verde proxies over the time period 1610-1995 A.D.58

Chapter 1: Introduction

OVERVIEW

The climate of the Earth is shaped by the composition and chemistry of the atmosphere. While it has long been known that the production of atmospheric gases occurs through various biological processes including photosynthesis, respiration, nitrification, and methanogenesis (Bowen, 1979; Griffin, 1979; Crutzen et al., 1986; Levine, 1991), research over the past few decades has identified another important biological phenomenon with profound and long-term effects on atmospheric composition: global biomass burning (Crutzen et al., 1979; Delmas, 1982; Delany et al., 1985). Global biomass burning (GBB) refers to the burning of the world's living and dead vegetation across different regions of the world, contributing a significant amount of greenhouse gases and pollutants to the atmosphere (Crutzen et al., 1979, Delmas, 1982; Delany et al., 1985; Anderson et al., 1988)—including as much as 40% of gross carbon dioxide and 38% of tropospheric ozone emissions annually (Andreae et al., 1996). These emissions in turn influence the climate system by changing the balance of incoming and outgoing solar radiation in the atmosphere, and by altering the albedo of earth surfaces at broad spatial scales. In addition, biomass burning contributes to the destruction of ozone and the production of acid rain (Anderson et al., 1988), affects the biogeochemical cycling of nitrogen, carbon, and water (Detwiler and Hall, 1988; Lobert et al., 1990; Levine, 1991), and perturbs the overall stability and composition of ecosystems around the world (Cunningham, 1963; Chandler et al., 1983; Goldammer, 1990; Debano et al., 1998). For these reasons, biomass burning is an important driver of global environmental change that must be understood by both scientists and policy-makers alike (Andrasko; 1991; Levine et al., 1995; Natural Resource Committee, 1999).

Although natural fires have existed since the evolution of land plants approximately 350-400 million years ago (Andreae, 1991), measurements of charcoal in dated lake sediment cores have shown a clear relationship between rates of burning and human settlement over the last 1.5 million years in many parts of the world (e.g., Pyne, 1982, Brain and Sillen, 1988; Pyne, 1997). Corollary pollen records documenting a shift in vegetation from pyrophobic to pyrotolerant species demonstrate the significant ecological impact of anthropogenic biomass burning (e.g. Johansson, 1963; Haberle 1998a; Haberle, 1998b; Larson and MacDonald, 1998; Haberle and Ledru, 2001; Dull, 2004a; Dull, 2004b). While human-induced fires have served a number of purposes throughout history, including forest clearing for agricultural use; pest, insect, and weed control; preservation of savannas and grazing pastures; hunting; nutrient mobilization; cooking and heating; and various other reasons (Lewis, 1973; Goldammer, 1988; Crutzen and Andreae, 1990; Pyne, 1998; Doolittle, 2000), the extent of anthropogenic burning has drastically increased over the past 100 years. Researchers suggest that up to 90% of fires worldwide now have anthropogenic sources, with this value expected to rise as human populations continue to grow (Levine et al., 1999). Recent quantitative studies documenting the geographic distribution of global fires indicate that most contemporary burning takes place in developing countries of the tropics at a rate more frequent and at greater spatial scales than previously estimated (Crutzen and Andreae, 1990; Hao et al., 1990; Andreae, 1991; Levine, 1995).

Because of the important contribution of tropical biomass burning to global environmental change, understanding fire regimes—the frequency, intensity, and types of fires—in tropical ecosystems is vital to our understanding of present-day climate variability (Levine et al., 1995). In order to contextualize current fire regimes, researchers have become increasingly interested in understanding *historic* burning

patterns and their environmental implications (Haberle et al., 1998; Natural Resource Committee, 1999; Haberle, 2001). While some studies have examined biomass burning in rainforests (Cochrane et al., 1999; Nepstad et al., 1999) and savannas (Scott, 1977; Roberts, 2000; Saarnak, 2001), one biome that has received relatively little attention in the published literature is tropical dry forest (TDF). This is true despite the fact that tropical dry forests are the most threatened forest formation globally, and home to the highest human population densities worldwide (Janzen, 1988).

In Central America, over 79% of people live in the TDF biome where fire is a common disturbance mechanism: seasonal droughts lead to desiccated fuel loads that provide favorable conditions for wildfire outbreaks at the end of the dry months (Murphy and Lugo, 1986). Although ignition sources are believed to be primarily anthropogenic, fire propagation potential is greatly influenced by the severity of annual drought conditions (Haberle, 2001). One mechanism known to affect meteorological conditions—and consequently, fire frequency and propagation—is the El Niño Southern Oscillation (ENSO), which causes widespread drought every 2-7 years in many parts of the world (Glantz, 1987; Glantz, 2001; Haberle, 2001). During an El Niño event, the surface water of the Pacific Ocean becomes warmer and alters trade wind patterns, which in turn influences temperature and precipitation regimes over many tropical locations. On longer timescales, variations in solar activity have been proposed to generate severe and synchronous drought in North America, South America, and the African Sahel at decadal- and centennial-scales (Hodell et al., 1995; Hodell et al., 2001; Van Buren, 2001; Schimmelman et al., 2003; Haug et al., 2003).

The largest expanse of Central American tropical dry forest stretches across Nicaragua's southern Pacific coast (Sabogal, 1992), which currently experiences devastating ENSO-induced drought during El Niño (negative) phases of the Southern

Oscillation (Glantz, 2001; Haberle, 2001), as well as a recent surge in fire activity (Koonce and Caban-Gonzalez, 1990; Natural Resource Committee, 1999). Although this region facilitates the study of historic fire regimes in tropical dry forests and their relation to short-term climate variability, few investigations exist (Suman, 1991)—particularly at a temporal resolution that fosters analysis of interannual- to interdecadal-scale changes in fire frequencies. The sole published study from Nicaragua’s Pacific coast is based on two low resolution marine sediment cores located ~100 km offshore (Suman, 1991); these records additionally span only the past 300-500 years and therefore do not adequately contextualize historic biomass burning in the country’s Pacific lowlands. The lack of paleo-fire research from Central American’s largest country leaves a significant spatial gap in paleoecological data that must be filled (Koonce and Caban-Gonzalez, 1990; Horn and Sanford, 1992; Haberle, 2001). Understanding natural patterns of fire occurrence in the Nicaraguan TDFs will facilitate management and preservation of this endangered forest biome.

In this study, I present a high resolution, 1,400-year record of biomass burning, sediment organic content, and watershed erosion reconstructed from a lake sediment core in Laguna Charco Verde, located on Ometepe Island within Lake Nicaragua (Fig. 1). The Laguna Charco Verde drainage basin is primarily covered by tropical dry forest, mirroring the adjacent mainland forest ecology of the Nicaragua Pacific lowlands. The data presented in this project are the first records of paleoenvironmental change recovered from within Lake Nicaragua, with an average sedimentation rate of 0.62 cm/year (1.60 years/cm); the Charco Verde data are thus unique in both location and resolution.

Using wavelet time-frequency analyses of reconstructed paleoenvironmental proxies in conjunction with regional climate records (Thompson et al., 1984; Hoyt and

Schatten, 1998; Stahle et al. 1998; Reimer et al., 2004) and archeological surveys (Lange, 1984; Haberland, 1986; Lange et al., 1992), I aim to identify both natural and anthropogenic sources of change in the fire record in order to document historic burning frequencies and their possible sources. Specifically, I attempt to relate natural periodicities within the fire record to paleo-ENSO events and/or variations in solar energy output, as well as to identify periods of prominent anthropogenic burning over the past 1,400 years. Wavelet transforms (e.g. Daubechies, 1992; Mallat, 1998) are a powerful means of analysis due to their ability to localize in time the different periodicities likely associated with human land use dynamics verses those of many climate mechanisms (Stanley et al., 2000; Keitt and Urban, 2005; Keitt and Fischer, 2006). While wavelets have been utilized in a variety of geophysical applications over the last decade (Kumar and Foufoula-Georgiou, 1993; Gamage and Blumen, 1993; Weng and Lau, 1994; Lau and Weng, 1995; Kumar et al., 1994; Baliunas et al., 1997; Fligge et al., 1999; Jevrejeva et al., 2003; Grinsted et al., 2004; Barrucand et al., 2006), they have not yet been employed to isolate natural signals in proxy records that may otherwise be obfuscated by anthropogenic activity. The macroscopic charcoal record, a proxy for historic fire frequencies, is one such indicator in which natural and human sources of change are greatly intertwined. I additionally conduct wavelet analysis on two other paleoenvironmental proxies—loss on ignition and magnetic susceptibility—in order to examine potential correlations between fire, fuel load, and erosion at various scales.

Because no baseline procedure for this wavelet application exists, a major goal of my study is to determine the best methodology for analyzing paleoproxy datasets, including the use of different wavelet functions and various preprocessing techniques. With this in mind, I seek to answer the following research questions about biomass burning and environmental change on Ometepe Island:

- 1) How do fire frequencies in Ometepe's tropical dry forests change over the past 1,400 years?
- 2) How is fire related to other indicators of environmental change on Ometepe Island?
- 3) How is the local record of biomass burning on Ometepe related to global short-term climate variability, specifically:
 - a. The El Niño Southern Oscillation at interannual scales; and
 - b. Fluctuations in solar activity at decadal and centennial scales?
- 4) How is the record of biomass burning related to anthropogenic activity and/or indigenous demographics as inferred from archeological surveys on Ometepe Island?

This study will thus provide insight into historic climate patterns and their affect on fire regimes and environmental change on Ometepe Island, thereby contextualizing current patterns of biomass burning in Nicaragua's Pacific lowland tropical dry forests.

ENVIRONMENTAL SETTING

Ometepe Island (11°0'24"N, 85°0'30"W) presents an opportunity to document the relationship between biomass burning, natural climate variability, and anthropogenic activity in a region where such analyses do not currently exist. The island has an area of 276 km² and consists of two stratovolcanoes joined by a narrow isthmus: the active Volcan Concepción (elevation 1,610 m) and the extinct/dormant Volcan Maderas (elevation 1,394 m) (Ometepe Biological Field Station, 2004). Ometepe formed in the late Quaternary when the regional axis of volcanism jumped southwestwards from the Tertiary volcanic range, depositing volcanic materials above a 1-km thick sequence of flat, lacustrine mudstones (van Wyk de Vries, 1996; Borgia and van Wyk de Vries,

2003). Although major eruptions have not been recorded at Maderas, volcanic activity from Concepción has been documented in 1883-1887 (active volcanism), 1908-1910, 1921, and 2007 (occasional ash emission), and 1948-1972 (fumarolic conditions) (Lange et al., 1992). Due to prevailing wind directions, tephra deposits dominate the western portions of Concepción, while lava primarily covers the eastern cone; dominant easterly winds also have generally precluded tephra deposition from ancient Maderas eruptions on Volcan Concepción (Borgia and van Wyk de Vries, 2003). Ometepe is primarily covered by patches of tropical dry forest and agricultural plots, with a cloud forest at the peak of Volcan Maderas. Mean annual temperatures range between 23°C and 28°C, and annual precipitation varies from 750 mm to 2500 mm with most rain falling during the pronounced wet season (May through October) (Berman et al., 2003; van Wyk de Vries, 2003).

Bimodal (wet and dry) seasonality in Central America is caused by the migration of the Intertropical Convergence Zone (ITCZ), an area of low pressure that forms where the northeast trade winds meet the southeast trade winds near the equator. The ITCZ migrates toward the area of most intense solar heating, moving towards the southern hemisphere from September through February and reversing direction for the northern hemisphere summer. Perturbations in ITCZ movement occur during El Niño events, during which the ITCZ is deflected south toward unusually warm sea surface temperatures in the tropical Pacific (Koonce and Caban-Gonzalez, 1990; Glantz, 2001). The lack of moist air over Central America during El Niño summer months results in severe drought in many parts of the region (Haug et al., 2003). Ometepe Island's dry season is thus exacerbated during El Niño years, which produce prolonged dry conditions at time scales of 2-7 years that result in greater burning potential due to desiccated fuel loads (Koonce and Caban-Gonzalez, 1990; Glantz, 1994; Glantz, 2001). Drought

conditions may also have the opposite effect on fire frequencies, however: extended periods of reduced precipitation may diminish the abundance of natural vegetation and agricultural crops, thereby critically reducing fuel loads and burning potential.

Fluctuations in solar energy output, which in turn affect sea surface temperatures and ITCZ migration, may also generate regional drought conditions. Research has suggested that synchronous drought across the Americas and parts of Africa on time scales of ~200 years—possibly caused by the ~206-year Suess cycle in solar activity—may have played a role in the collapse of the Maya civilization in the Yucatan Peninsula (Hodell et al., 1995; Hodell et al., 2001; Van Buren, 2001; Schimmelmann et al., 2003; Haug et al., 2003). Because the sun’s energy output fluctuates at high frequencies in addition to centennial scales (e.g., the 11- and 22-year Schwabe and Hale periodicities, respectively), variations in solar activity may also influence Central American climate and the fire regimes of Nicaragua’s tropical dry forests. Climate variability at ENSO- and solar activity-relevant time scales are investigated in this project in order to document possible short-term climate forcing of fire regimes.

CULTURAL HISTORY

Ometepe Island has been inhabited by indigenous communities that practiced agricultural activities—including the use of fire as a land management tool—for thousands of years (Haberland, 1986). The island is located within the “Greater Nicoya Archaeological Subarea” (Norweb, 1964), a region encompassing northwestern Costa Rica and Pacific Nicaragua and identified by a distinctive and common ceramic tradition among disparate indigenous communities. Positioned between the Mayan cultures to the north and the Intermediate Area traditions to the south, the cultural affinity of the Greater Nicoya has long been debated (Willey, 1966; Baudez, 1970; Stone, 1977; Lange 1984;

Lange et al., 1992): should the Greater Nicoya be considered a subregion of Mesoamerica or the Intermediate Area societies, or do the Nicoya stand apart from their northern and southern neighbors? Recent research has postulated that the latter position is most likely correct, with the imperial civilizations largely “neglecting” the Greater Nicoya “transition zone” due to a lack of opportunity for natural resource exploitation (Lange et al., 1992). Although the Greater Nicoya subarea did not exist as one unified tradition, research suggests that large local populations and a strong cultural authority were able to preserve Nicoyan autonomy (Lange, 1984; Haberland, 1986; Lange et al., 1992).

Original settlement of Ometepe Island between 2000-1500 B.C. is thought to have been facilitated by the island’s highly fertile soils, which fostered intensive agricultural activity for at least three millennia prior to Spanish arrival. Changes in climate and volcanic hazards likely affected the cultural development and population of Ometepe’s indigenous communities, which evolved through time with sporadic migrations from the mainland (Haberland, 1986; Lange et al., 1992). Archeologists working on Ometepe have identified nine cultural phases of settlement and subsistence on Ometepe Island that can be combined into four larger periods, summarized in Table 1 (Haberland, 1986; Lange et al., 1992). Overall, the abundance of human artifacts on the western side of the island suggests historically greater occupation and land use on Volcan Concepción than on Volcan Maderas (Haberland, 1986). The following description of archeological findings on Ometepe Island is summarized from Haberland (1986) and Lange et al. (1992).

The earliest phase of human occupation on Ometepe Island has been identified by subsistence activities along the base of Volcan Concepción. Ometepe’s inhabitants during the Dinarte (2000 – 500 B.C.) and Angeles (500 – 200 B.C.) phases are believed to have engaged in farming, hunting, and fishing; these two phases, split by a volcanic

eruption around 500 B.C, represent the first greater period of cultural development on Ometepe Island. The second period of development is comprised of the Sinacapa (200 B.C. – 1 A.D.), Mantiel (1 A.D. – 500 A.D.), and San Roque (500 A.D. – 950 A.D.) phases. The Sinacapa Phase marks the earliest record of settlement on Maderas, as well as the first material evidence of maize cultivation with the findings of molcajetes (mortar and pestle) and manos (groundstones). Archaeological evidence also suggests an influx of new settlers to the island with the introduction of three new ceramic traditions. Faunal remains consistent with fishing and hunting activities are present during the Mantiel phase, which ended with volcanic activity and partial abandonment of the island. The San Roque Phase is characterized by a rise in the numbers of manos and metates, faunal remains, and turtle bones, suggesting the return of the island's population. Primary burials throughout the island also peaked during the San Roque Phase, representing the pinnacle of cultural development on Ometepe Island.

The third period of prehistoric occupation on Ometepe is comprised of the Gato (1000 A.D. – 1200 A.D.), La Paloma (1100 A.D. – 1300 A.D.), and San Lazaro (1300 A.D. – 1400 A.D.) phases. An increase in groundstones, as well as the presence of mainland ceramic traditions, suggests the influx of new migrants to the island during this time. The San Lazaro Phase is identifiable by only one survey site located on a series of old beach gravels at the southern flank of Concepción, signifying a drop in Lake Nicaragua water levels that may have contributed to the lack of San Lazaro artifacts. The Santa Ana phase (1400 A.D. - 1550 A.D.) is last pre-Conquest period on Ometepe Island, with new ceramic traditions suggesting the arrival of migrants from the Atlantic coast of lower Central America before Spanish contact in 1522.

Ometepe was annexed via settlement by Spanish conquistadors at the end of the 16th century. The island was hard hit by pirates through the late 17th century, who

erected settlements on Ometepe's shores and clashed with indigenous populations—local communities are believed to have moved to higher elevations on the volcanoes to avoid European contact. Today, the most important villages on Ometepe are Moyogalpa and Altagracia, with an economy is based upon tourism, livestock, and the production of export crops such as coffee, cotton, and bananas (Parker, 1964).

PROJECT SUMMARY

The physical geography and cultural history of Ometepe Island facilitates the examination of historic climate variability, anthropogenic activity, and their affect on fire regimes and environmental change, thereby contextualizing current patterns of biomass burning in Nicaragua's Pacific lowland tropical dry forests. This study is organized into four chapters. **Chapter I** provided an introduction to the project in relation to the existing body of related literature, and detailed the environmental setting and cultural history of Ometepe Island. **Chapter II** explores the literature that informs this study in depth, including the fields of paleoclimatology, paleoecology, and geophysical wavelet applications. **Chapter III** details he methods employed in this project—the macroscopic charcoal proxy and wavelet power and coherency analyses—and provides an overview of project results. **Chapter IV** discusses the significance of proxy record reconstructions and wavelet analyses, relating project results to the broader scientific community, as well as summarizing specific conclusions presented by this study.

Chapter 2: Literature Review

The scientific literature informing this study incorporates three important research fields that examine Earth's environmental history. *Paleoclimatology* investigates prehistoric climate at various time scales using a variety of proxy evidence. Through documenting the relationship between fire frequencies and short-term climate variability in southwestern Nicaragua, I investigate local biomass burning patterns as they relate global interannual, interdecadal, and centennial climate forcing mechanisms, specifically ENSO and variations in solar energy output. The relationship among organisms, including humans, and their past environment is explored by investigations in *paleoecology*. Through multiple proxies, this project provides a high-resolution analysis of anthropogenic environmental modification (sediment organic content, erosion, and biomass burning) in southwestern Nicaragua, a region where detailed environmental histories do not exist. I also provide the first account of the relationship between the Nicoya indigenous community and environmental change in southwestern Nicaragua through the comprehensive comparison of fire frequencies, paleovegetation abundance, erosion, climate variation, and archeological surveys from Ometepe Island. Finally, *wavelet analysis of geophysical data* is a rapidly growing methodology for the examination of environmental time series. I apply wavelet transforms to paleoproxy datasets in order to document natural forcing in records potentially obfuscated by anthropogenic activity, thereby contributing a novel application of wavelet techniques to this body of literature.

1. PALEOCLIMATOLOGY

In the early 1830s, Charles Lyell's advocacy of the principle of uniformitarianism, the idea that the same geological process operating today also did so in the distant past (Lyell, 1830-1833), fundamentally changed how scientists viewed the Earth. The acceptance of uniformitarianism implied that slow-moving processes over millions of years were the primary shapers of Earth's surface, as opposed to originating instantaneously at some point in the relatively recent past (as purported by the principle of catastrophism). The recognition that the planet was more than a few thousand years old generated corollary questions about Earth's historical climate at time scales greater than ever previously conceived, thus leading to the birth of paleoclimatology as a scientific discipline. The field of paleoclimatology was further advanced after the occurrence of two major scientific developments in the early nineteenth and twentieth century, respectively: 1) The acceptance that one or more "ice ages" existed in the past, where a massive polar ice sheet blanketed large portions of Europe and North America (Agassiz, 1840); and 2) that such ice ages are caused by slight changes in Earth's orbital parameters: eccentricity, tilt, and precession (Milankovitch, 1938). Subsequent twentieth century research has shown that the Pleistocene Epoch (approximately 1.65 million years – 10,000 years before present (B.P.)) featured 18 expansions of ice over Europe and North America (Imbrie and Imbrie, 1980).

One of the most important advances of the last few decades is the discovery that the Earth's climate has varied rapidly and repeatedly on sub-glacial time scales (Denton and Karlen, 1973; Broecker et al., 1988; Dansgaard et al., 1993; Bond et al., 1993; Bond and Lotti, 1995; Bond et al., 1997; Alley et al., 2003). Historically perceived as a relatively static period in Earth's climate history, the Holocene Epoch (~10,000 years B.P. through the present) is now viewed as remarkably dynamic: evidence of the 8,200

year cold event, the Medieval Warm Period (800-1200 AD), and the Little Ice Age (1250-1850 AD) from Eurasia and North America particularly document high frequency climate fluctuations (Boyle and Keigwin, 1987; Broecker et al., 1990; Stuiver et al., 1995). Although the drivers of these centennial-scale climate events are still being debated, researchers have invoked fluctuations in the sun's energy output on timescales from days to millennia as a potential, if partial, cause. Important periodicities and quasi-periodicities in solar activity include cycles of approximately 11, 22, 55, 88, 208, 232, and 400-500 years (Rind, 2002; Moussas et al., 2005).

On yet shorter time scales, the discovery of the El Niño Southern Oscillation (ENSO), or the disruption of Earth's ocean-atmosphere system every 2-7 years that causes drastic disturbances in weather patterns across the globe, affixes yet another element of complexity to Earth's climate system. While ENSO events were seen as a largely local phenomenon for much of the 20th century restricted to the Peruvian Pacific coast, the global incidence and severity of the 1972-73 El Niño triggered an upsurge of scientific research into present and historic ENSO cycles (Glantz, 1994; Glantz, 2001; Haberle, 2001; Caviedes, 2001). Severe, synchronous droughts in various regions around the world are one of the most prevalent and devastating characteristics of today's ENSO regime (Glantz, 2001). These droughts have been linked to increased global fire activity that endangers property, affects forest ecology (Koonce and Caban-Gonzalez, 1990; Debano et al., 1998; Siegert and Hoffmann, 2002), and causes the release of massive amounts of greenhouse gases into the atmosphere (Crutzen et al., 1979; Delmas, 1982; Delany et al., 1985; Andreae and Crutzen, 1990; Andreae, 1996; van der Werf, 2004).

Using the derived natural periodicities within the record of biomass burning as a proxy for severe drought frequencies on Ometepe Island, I will document natural climate variability in southwestern Nicaragua. This record is compared to regional- and

hemispheric-scale proxies of ENSO and solar activity in order to investigate the temporal correlations between natural forcing mechanisms, precipitation anomalies, and fire activity on Ometepe Island.

2. PALEOECOLOGY

Paleoecologists attempt to use various proxy data to define the structure and function of past ecosystems and to document their evolution through time. While the roots of paleoecology naturally coincide with insights into Earth's dynamic climate, the discipline was propelled forward in the mid-1900s with the discovery that fossil pollen from different layers of buried sediments was an accurate and feasible means of reconstructing historic changes in vegetation (von Post, 1946). Over the past century, the comparison of Quaternary fossil pollen assemblages from lake sediment cores with modern compositions (palynology) has allowed paleoecologists to infer and reconstruct the makeup of different vegetation communities around the world (e.g. Ikuse, 1956; Heusser, 1971; Birks and Gordon, 1985; Faegri and Iverson, 1989; Moore et al., 1991; Knapp et al., 2000). When analyzed in conjunction with other paleoenvironmental indicators such as the macroscopic charcoal, loss-on ignition (LOI) and magnetic susceptibility (MS) proxies—documenting historic fires, vegetation abundance, and watershed erosion, respectively—histories of regional environmental change through time may be produced in detail (Dean, 1974; Mullings, 1977; Dearing, 1999; Heiri et al., 1999; Sandgren and Snowball, 2001). An overview of these paleoenvironmental proxies is provided at the end of this section.

As the development of paleoecology coincided with a growing number of paleoclimate records, researchers began to analyze environmental variability in the context of climate change through time (e.g. Horn and Sanford, 1992; Brenner et al.,

1993; Hodell et al., 1995; Sluyter, 1997; Leyden et al., 1998; Behling and Colinvaux, 2000; Hodell et al., 2001; Neff et al., 2005). Although these analyses provide excellent regional investigations into historic ecosystem evolution and response to climate dynamics, such studies are inherently limited to local or regional scales usually determined by the size of the lake drainage basin from which the sediment cores were extracted. The advent of supercomputers in the 1970s, however, facilitated the application of climate models to problems of paleoecology, thus allowing paleoecologists to map vegetation across the globe since the last glacial maximum at various snapshots through time and with a multitude of climatic parameters (COHMAP members, 1988). Such terrestrial models continue to require regional, paleoproxy analyses in order to validate model results and to provide more detailed examinations of vegetation change at shorter temporal and smaller spatial scales (Birks and Gordon, 1985; Horn and Sanford, 1992; Haberle, 2001; Natural Resource Committee, 1999).

In the past few decades, environmental histories have become increasingly analyzed in the context of archeological and anthropological records of human land use activities. Investigators continue to debate the degree of modification that native peoples may have exerted on their landscape (Sauer, 1956; Stewart, 1956; Denevan, 1992; Vale, 2002). Did the earliest European settlers find an undisturbed wilderness—a “pristine landscape”—largely untouched by the “ecological Indian” (Sale, 1990), or had Native Americans already left a profound and pervasive environmental footprint—a “humanized landscape”—via their agricultural, clearing, burning, and other actions (Lewis, 1973; Pyne, 1998; Doolittle, 2000)? Although fire is a natural disturbance agent in many ecosystems (Kellman and Meave, 1997; DeBano et al., 1998; Cochrane et al., 1999), some have argued that the alteration of fire frequencies and magnitudes by anthropogenic activity may have had profound impacts on the landscape, including the modification of

natural vegetation communities (Sauer, 1956; Stewart, 1956; Koonce and Caban-Gonzalez, 1990; Sampaio et al., 1993; Dull, 2004b;), overall vegetation abundance (Nepstad et al., 1999; Laurance and Williamson, 2001), and increased erosion (Meyer et al., 1992; Pierce et al., 2004). Records of historic fire frequencies are thus integral to our understanding of the human-environment relationship and our ability to assess anthropogenic environmental impacts through time and space.

Paleoecological research in Central America to date has focused on pollen and charcoal reconstructions from lake sediment cores in Mexico (Hodell et al., 1995; Sluyter, 1997; Leyden et al., 1998; Hodell et al., 2001; Hodell et al., 2005; Neff et al., 2005), Guatemala (Brenner et al., 1993), El Salvador (Brenner et al., 1990; Dull, 2004a; Dull, 2004b), Panama (Bush, 1994; Behling and Colinvaux, 2000), Costa Rica (Horn and Sanford, 1992; Horn, 1993; Clement and Horn, 2000; League and Horn, 2000; Anchukaitis and Horn, 2005), and the Nicaraguan Pacific Basin (Suman, 1991), but researchers have yet to explore the largest Central American lacustrine environment, Lake Nicaragua. Furthermore, historical fire regimes have not been adequately explored in the tropical dry forest biome, the most endangered tropical biome globally and home to the highest human population densities worldwide (Murphy and Lugo, 1986; Janzen, 1988). Current studies additionally do not provide a temporal resolution that fosters analysis of ecological variability driven by sub-centennial scale climate change.

Through the evaluation of fire frequencies over the past 1,400 years and comparison to proxy evidence of watershed erosion and vegetation abundance, this study will provide a historical perspective on the disturbance regime on Ometepe Island. Further comparison to climate records and archeological surveys will provide insight into the relationship between ecological disturbance, short-term climate variability, and broad trends in indigenous demographics through time.

Overview of Paleoproxies

Macroscopic Charcoal

Charcoal is produced by the incomplete combustion of organic matter; charcoal particles embedded in lake sediments were produced during different fires and deposited via eolian or hydrologic processes from local or regional sources. The amount of charcoal found in a sediment core is therefore a function of the characteristics of the fire, the amount of available biomass (fuel), and the processes of charcoal transport (Whitlock and Larson, 2001). In a well dated core where the method of charcoal production, transport, and deposition have been carefully investigated, the quantification of charcoal particles in contiguous sediment strata can be used to determine historical variations in fire intensity and frequency in a watershed area. While researchers may utilize different sized charcoal particles in their analyses of fire regimes, this investigation quantifies macroscopic charcoal (>150 μm) particles from sieved sediments, as the larger size of these particles generally improves the accuracy of determining a fire source area and time of deposition (Whitlock and Larson, 2001).

Loss on Ignition

The percentage of organic matter in lakebed sediments through time is a proxy for overall vegetation abundance in a watershed (Dean, 1974). High sediment organic content suggests a relatively stable climate conducive to vegetation growth with few erosional episodes, while low sediment organic content suggests landscape instability and increased erosion caused by natural and/or anthropogenic disturbance. The loss-on-ignition proxy is determined by weighing sediment before and after subjecting the material to temperatures at which organic carbon will combust, where sample size,

exposure temperature and time, and measurement techniques are held constant for all samples (Heiri et al., 1999).

Magnetic Susceptibility

Lakebed sediments are comprised primarily of inorganic minerals eroded and transported from the surrounding watershed (Sandgren and Snowball, 2001). These minerals can be classified based upon their response to magnetism, or their “magnetic susceptibility” (Mullings, 1977; Sandgren and Snowball, 2001). Magnetic susceptibility data is used as a proxy for environmental instability, specifically as an indicator of relative rates of erosion. A stable environment suitable for vegetation growth will yield a lower ratio of inorganic to organic matter in lakebed sediments (low magnetic response) than will a highly variable environment in which erosion is a dominant force on the landscape (high magnetic susceptibility values) (Dearing, 1999).

3. WAVELET ANALYSIS OF GEOPHYSICAL DATA

Wavelet transform analysis is rapidly becoming a common technique for analyzing nonstationary time series, where variations of power are localized at different frequencies through time. Wavelets were developed to overcome shortcomings of the Fourier transform, which decomposes a signal using a constant resolution at all frequencies and cannot provide localized information regarding dominant modes of variation in a time series. The use of the multiresolution technique (Mallat, 1989) in which a time series is analyzed with different resolutions at multiple scales and decomposed into time-frequency space facilitates the localization of both the primary frequencies in a signal as well as their temporal evolution.

Wavelet transformation analysis is conducted by repeatedly performing the convolution operation of a time series and a “mother” wavelet as the wavelet function is translated (shifted) through the record by parameter τ and scaled (dilated or compressed) by parameter s . The translation parameter describes the temporal location of the wavelet function as it is moved through the signal, while the scale parameter, defined by frequency⁻¹, either dilates or compresses a signal and thus identifies high and low frequencies throughout the time series (Foufoula-Georgiou, 1993; Kumar and Foufoula-Georgiou, 1994; Torrence and Compo, 1998). While numerous mother functions exist, each must meet two conditions in order to be “admissible” as a wavelet: 1) the mean of the wavelet must be zero; and 2) the wavelet must be localized in time and frequency space (Farge, 1992). Choosing a mother wavelet for the transformation of a time series is based upon multiple characteristics associated with that function, including its shape, width (e-folding time of the wavelet amplitude), complex or real components, and orthogonal versus nonorthogonal wavelet basis (Kumar and Foufoula-Georgiou, 1993; Torrence and Compo, 1998).

Wavelet coherency is the “wavelet domain equivalent” (Maraun and Kurths, 2004) of the correlation function (the normalized wavelet cross spectrum), measuring the linear relation between two processes with respect to time and scale. A value of one implies a perfect linear relation, while a value less than one indicates that either a perfect linear relation is disturbed by noise, or that the relationship is non-linear. Because nonzero values of coherency may still arise even when two time series are unrelated, significance tests must be performed to estimate the probability distribution of coherency under H_0 , the null hypothesis (no relationship) (Kumar and Foufoula-Georgiou, 1993; Torrence and Compo, 1998; Maraun and Kurths, 2004). Wavelet coherency analysis thus

provides a robust statistical measure of the covariance between two signals at various times and scales that are not necessarily apparent in time series data.

Within geophysics, applications of wavelet techniques include the detection of energy cascades and coherent structures in the atmosphere; remotely sensed hydrometeorological and geological variables for data compression; seismic wave propagation and structure analysis; detection of scale-specific community and population dynamics; and space-time analysis of various climate indices, among others (e.g. Gamage and Blumen, 1993; Weng and Lau, 1994; Kumar et al., 1994; Baliunas et al., 1997; Torrence and Compo, 1998; Fligge et al., 1999; Grinsted et al., 2004; Keitt and Urban, 2005; Keitt and Fischer, 2006). In wavelet applications to climate studies in particular, researchers attempt to identify dominant forcing mechanisms in direct and/or proxy datasets at multiple scales (e.g. Kumar and Foufoula-Georgiou, 1993; Lau and Weng, 1995; Jevrejeva et al., 2003; Barrucand et al., 2006). Wavelets are a powerful tool in such analyses, as common features in the time-frequency characteristics of two time series may be identified despite large differences in time series fluctuations due to local conditions (Lau and Weng, 1995; Torrence and Compo, 1998; Barrucand et al., 2006). Researchers are thus able to attribute variations in time series data to external forcing mechanisms at both high and low scales, including orbital and solar cycles, ENSO events, and/or other weather and climate anomalies.

In addition, because many climate mechanisms have a different time-frequency signature than human activity (e.g., anthropogenic burning is not believed to mirror the exact periodicities of climate cycles), wavelet analysis of paleoenvironmental proxies may help extricate natural from anthropogenic sources of change in time series data when the two contribution sources are intertwined. High wavelet power, indicating similarity between the time series data and the cyclic wavelet mother function, may suggest periods

of strong climate forcing, while periods of low power may indicate signal dominance by less-periodic anthropogenic disturbance. The utilization of wavelet techniques for this purpose is a novel application that may serve as a model for future analyses of paleoproxy data with a combination of natural and anthropogenic contributions to time series variability.

SUMMARY

This project makes significant contributions to the fields of *paleoclimatology*, *paleoecology*, and *wavelet analysis of geophysical data*. Through the construction and comparison of records of biomass burning, loss on ignition, magnetic susceptibility, and regional climate proxies, this study documents the historic relationship between drought, fire, and environmental change in the tropical dry forests of southwestern Nicaragua. This study additionally provides a high-resolution environmental history of an endangered ecosystem requiring a historical perspective on natural disturbance and anthropogenic environmental impacts. In addition, the utilization of wavelet transform analysis to extract natural periodicities from paleoproxy records is a wavelet application that has yet to be utilized in paleoecological and paleoclimatological research, and may serve as a model for future analyses.

Chapter 3: Methods and Results

METHODS

This project reconstructs the fire history of Ometepe Island through the analysis of a lake sediment core extracted in July, 2004 by the research team of Dr. Robert Dull (University of Texas at Austin). The core measures 6.38 meters in length and was taken from Laguna Charco Verde, located at the southern base of Volcan Concepción at an elevation of 30 m (Fig. 1). The core was split and analyzed for stratigraphy, inclusions, and color and sub-sampled at 2-cm intervals at the Quaternary Paleoecology Laboratory at the University of Texas at Austin. Radiocarbon (^{14}C) dates were obtained for six samples from the Keck-CCAMS laboratory at the University of California at Irvine in order to construct an accurate, high-resolution core chronology. Radiocarbon years were converted to years AD via the CALIB program (Stuvier et al., 1998).

Charcoal analysis was performed every 2-cm on 1.25 cc of sediment from the Charco Verde core. In order to facilitate the breakdown of highly cohesive clay particles around charcoal fragments, samples were soaked for 24 hours in a 5% sodium hexametaphosphate deflocculant solution. Each sample was then rinsed with distilled water through a 150 μm sieve, and charcoal particles were counted from the >150 μm fraction at 20X magnification; charcoal counts were converted to charcoal concentrations (particles per cc). In order to mitigate the effects of potentially spurious peaks in the charcoal record, charcoal accumulation rates (CHAR), calculated as charcoal concentration per cm^2 per year, were additionally computed. However, while the averaging affect of CHAR calculations was desirable for time series comparisons, charcoal accumulation rates were undesirable for wavelet analysis because they reduce

the magnitude and resolution of charcoal fluctuations. Wavelet analyses were therefore employed on the charcoal concentration data rather than charcoal accumulation rates.

The macroscopic charcoal data were compared to loss on ignition and magnetic susceptibility analyses, also performed at a 2-cm resolution. The loss-on-ignition (LOI) proxy is determined by weighing sediment before and after subjecting the material to temperatures at which organic carbon will combust, where sample size, exposure temperature and time, and measurement techniques are held constant for all samples (Heiri et al., 1999). In this study, organic content was measured every 2 cm by percent dry weight loss on ignition after 2 hours in a 550° C in a Barnstead Thermolyne furnace. Magnetic susceptibility (MS) readings were taken every 2 cm for the Charco Verde core using a Barrington MS2 magnetic susceptibility meter and a Barrington MS2B magnetic susceptibility sensor. The average of three magnetic susceptibility readings was documented and recorded as volume magnetic susceptibility (k).

This project implemented wavelet transform analyses to determine the dominant frequencies, localized in time, embedded within the charcoal, LOI, and MS proxy records. Paleoproxy time series and wavelet power spectra were then compared to wavelet transformation of four regional climate records: two paleoproxy records of short-term climate variability were used in order to facilitate comparisons over the entire time series, and two reconstructions of direct indicators of ENSO and sunspot cycles were compared over their respective periods of record. The long-term climate proxies utilized by this study include: 1) Quelcayya ice core snow accumulation rates, a proxy for paleo-ENSO cycles years over ~1300 years (Thompson et al., 1984); and 2) North American $\Delta^{14}\text{C}$ concentrations, a multi-millennia proxy for variations in solar energy output (Reimer et al., 2004). The Charco Verde records were additionally compared to the following short-term climate indicators: 1) the experimental dendroclimatic

reconstruction of winter Southern Oscillation Index (SOI) over the period 1706-1997 A.D. (Stahle et al., 1998); and 2) annual average group sunspot number (SN), a reconstruction of sunspot cycles, over the period 1610-1995 A.D (Hoyt and Schatten, 1998). Comparisons were made through wavelet coherency analyses in order to quantify the relationship between regional climatic oscillations and environmental change at Ometepe Island through time, and two types of significance tests were performed: a point-wise test that examines every data point against H_0 of no correlation, and an area-wise test that also accounts for the size and geometry of coherent patches. The latter test is considered to be more conservative, as it eliminates possible spurious peaks caused by the problem of multiple testing (Maraun and Kurths, 2004). Both tests were performed on all wavelet analyses undertaken in this project (e.g., both wavelet power and coherency) at a significance level of 0.05; wavelet power and coherency peaks are therefore considered significant at the 95% confidence level.

A major goal of this study was to determine the best methodology for extracting climate signals from paleoproxy records, as wavelets have not yet been used in this capacity in current published literature. As a preliminary analysis, this project examined three mother wavelets (Daubechies, Difference of Gaussian (DOG), and Morlet) in order to document any significant discrepancies that arose due to the use of different wavelet functions. The Morlet and DOG functions are continuous wavelet transforms (CWTs), which operate at every scale from a minimum value given by the Nyquist criterion (2ω radians, where ω is the highest frequency in the signal) (Kumar and Foufoula-Georgiou, 1994). By contrast, the Daubechies wavelet is a discrete wavelet transform (DWT), where calculations are made only on a set of scales and positions based on powers of two

(dyadic) using the Mallat algorithm¹ up to the 2^n value closest to half the length of the time series (Mallat, 1989).

All three wavelets tested identified the periodicities at similar scales and temporal locations, with the only significant differences lying in the resolution of peak wavelet power. The Morlet wavelet transform was chosen as superior due to its ability to localize time and frequency both sufficiently and relatively evenly. The Charco Verde and regional climate proxy data were thus analyzed by the Morlet transform in three ways in order to determine the best way to extract natural periodicities and to document any discrepancies arising from different preprocessing procedures: 1) as raw time series data; 2) after preprocessing with a bandpass filter of 2-32 years, which concentrates wavelet power at the higher frequencies of interest; and 3) and after bandpass filtering log-transformed time series data, which reduces heteroskedasticity that may bias wavelet results. Data was interpolated at a constant time-step of 1 year for each time series in order to account for differences in sedimentation rates throughout the core. All analyses were implemented using the R statistical software package (Ihaka and Gentleman, 1996) with modified code from supporting packages Rwave (Carmona et al., 1998) and Sowas (Maraun and Kurths, 2004).

Appendices A1-A3 contain the wavelet power spectra of the charcoal, LOI, and MS data, respectively, after analysis as 1) raw time series; 2) bandpass filtered at 2-32 years, and 3) bandpass filtered (2-32 years) log-transformed data. Appendices B1-B3 illustrate results for wavelet coherency analyses between the charcoal - LOI, charcoal - MS, and MS - LOI records as 1) raw time series, and 2) bandpass filtered at 2-32 years (log-transformed data produced the same results in coherency analyses). Appendices C1-

¹ The Mallat algorithm decomposes the signal with successive lowpass and highpass filters, where the high pass filter produces detailed information and the lowpass filter produces coarse information at each level of analysis.

C4 document wavelet coherency analyses between the charcoal record and each regional climate reconstruction used in this project (Quelcayya snow accumulation, SOI, $\Delta^{14}\text{C}$, and group sunspot number) after processing as: 1) raw time series; 2) bandpass filtered at 2-32 years, and 3) bandpass filtered (2-32 years) log-transformed data. As evident in Appendix A, significant wavelet peaks primarily occurred at scales less than ~ 64 years with the most prominent periodicities at less than ~ 32 years, thus precluding analysis of centennial-scale climate change in the Charco Verde records. Preprocessing by a 2-32 year bandpass filter successfully increased wavelet power at the interannual and decadal scales of interest, but this procedure did not reduce the heteroskedastic bias in the time series data (evident by local concentration of wavelet power at higher scales as a response to overall time series trends). Log transformation of the original time series data reduced this bias, concentrating power at low scales and eliminating spurious peaks resulting from unequal data variance. This methodology was thus chosen as superior, and all subsequent analyses are implemented using the log-transformed, 2-32 year bandpass filtered wavelet results.

RESULTS

Time Series Data

Table 2 details radiocarbon sampling and age calibration results, while Fig. 2 illustrates the age-depth relationship of the Charco Verde lake sediment core. The time period of analysis spans the past 1423 years, corresponding with a core bottom age of 581 A.D. Sedimentation rates vary between 0.23 and 1.91 cm/year (0.52 - 4.35 years/cm), with an average sedimentation rate of 0.62 cm/year (1.60 years/cm) and a corresponding mean sampling resolution of 3.20 years. The highest frequency capable of extraction by

wavelet analysis thus ranges between 1.04 and 8.70 years, with an average of 6.40 years; this frequency corresponds with the upper range of ENSO variability.

Figure 3 illustrates the fluctuations in a) charcoal accumulation rates (CHAR), b) charcoal concentrations, c) loss on ignition (LOI), and d) magnetic susceptibility (MS) at Charco Verde over the period of record. CHAR is at its highest value (440 particles/cc/year) at 581 A.D., and falls by approximately an order of magnitude between 581 and 900 A.D. and again at ~1500 A.D., where CHAR variability additionally dwindles with values $< \sim 10$ particles/cc/year (Fig. 3a; note the log scale). These changes in charcoal accumulation rates are mirrored by raw charcoal concentration values (Fig. 3b). Macroscopic charcoal concentrations range from 6-781 particles/cc and significantly vary throughout the core at both fine and coarse scales; highest values occur between 1100-1300 A.D and 581-700 A.D., with continuous charcoal depletion (< 30 particles/cc) after ~1500 A.D (Fig. 3b). Both the charcoal and CHAR results indicate periods of increased burning between 581-800 A.D. followed by a reduction in fire activity until ~1100 A.D., when charcoal values reach their peak and subsequently decline after 1300 A.D.

The LOI and MS time series indicate an expectedly inverse correlation, with low sediment organic content ($\sim 5\%$) and high erosion (MS values $> \sim 100$ k) persisting from 581-1000 A.D (Figs. 3b-c). At this point, the magnetic susceptibility data values drop and remain low throughout the record ($< \sim 45$ k), with the least magnetic responses occurring between 1000-1150 A.D. and 1300-1400 A.D (values of 5-10 k; Fig. 3d). LOI values, by contrast, experience a rapid rise to 30% organic content at 1000 A.D. with sustained values through 1100 A.D. The proxy remains relatively stable from 1000-1750 A.D., when LOI rapidly rises and falls through a 100-year period (up to 58% organic content) before returning to stable values at approximately 1850 A.D. (Fig. 3c).

Wavelet Transform Analysis

Charco Verde Wavelet Power Spectra

Figure 4 illustrates wavelet power spectra (WSP) for each log-transformed and bandpass-filtered time series; wavelet power peaks for each Charco Verde proxy are summarized in Table 3. Figures are zoned by Ometepe archeological horizons (Haberland, 1986) to indicate long-term trends in indigenous demographics and cultural development. The charcoal WSP displays high power after ~1500 A.D. at scales of 2-8, 10-17, and 21-28 years. Particularly noteworthy is the prevalence of power at ~7-, 11-, and 22-year periodicities corresponding with the upper end of ENSO variability and two prominent sunspot cycles, thus suggesting a relationship between short-term climate forcing and fire regimes in the Ometepe TDFs. Peak power at a scale of ~15 years may correspond with variability within or the interference between these forcing mechanisms. Additionally significant peaks occur at 800-1000 A.D. at a scale of 10-14 years, 750-850 A.D. at 2-8 years, and 600-775 A.D. at 21-31 years. The LOI WSP (Fig. 4b, Table 3) demonstrates periods of high wavelet power at similar, climate-relevant scales: from 1940-1980 A.D at a scale of 8-12 years, 1600-1800 A.D. at 8-13 years, 1300-1400 A.D. at 2-32 years (with peak concentration between 10 and 22 years), 800-1000 A.D. at 11-16 and 22-32 years, 750-850 A.D. at 2-10 years, and 590-650 A.D. at 14-20 years. In contrast to the charcoal and LOI records, however, the magnetic susceptibility WSP indicates fewer significant peaks (Fig. 4c, Table 3): 1750-1850 A.D. at scales of 10-13 and 16-22 years, 850-1000 A.D. at 19-32 years, and 750-850 A.D. at 2-32 years (with peak concentration at 6-11 years).

Charco Verde Wavelet Coherence

Figure 5 illustrates wavelet coherence analyses between the proxy records: a) charcoal - LOI; b) charcoal - MS; and c) MS - LOI. Wavelet coherence peaks for each Charco Verde proxy are summarized in Table 4. Because each environmental proxy is a function of numerous local conditions, coherent peaks within these data suggest a common forcing mechanism driving variations at similar times and scales. Particularly notable are the covariances between each record at 1) 581-700 A.D. at scales of 2-7 years, 2) 850-900 A.D. at 2-7 and 10-12 years, 3) 1025-1150 A.D. at 2-6 and 7-11 years, and 4) 1300-1350 A.D. at 2-7 years. The charcoal and LOI records are also continuously coherent after ~1500 A.D. at scales of 2-7 years, with additional peaks at 2-11 and 18-22 years between 1750 and 1850 A.D. (Fig. 5a). Coherency between the charcoal - MS and the LOI - MS proxies generally does not exceed a scale of 7 years after ~1400 A.D. (Figs. 5b-c).

Comparison to ENSO Reconstructions

Time series and WSP results over the period of record of the Quelcayya ice core (1256-1984 A.D.) are illustrated in Figure 6, while wavelet coherence results between Quelcayya snow accumulation and Charco Verde a) charcoal, b) LOI, and c) MS are depicted in Figure 7. Peak wavelet power and coherencies are summarized in Tables 3 and 4, respectively. The Quelcayya WSP indicates significant power at ENSO frequencies throughout the record, as well as concentrations of power centered around 22 years at 1600-1700 A.D., 1300-1400 A.D., 900-1100 A.D., and 775-850 A.D.; the Quelcayya record may thus also respond to variations in solar activity in addition to ENSO forcing. Although the Quelcayya ice core data demonstrate limited covariance with the Charco Verde proxies at the 95% confidence level, coherent peaks exist throughout each proxy at ENSO-relevant scales (Figs. 7a-c). In particular, coherency

between the Quelcayya and charcoal record (Fig. 7a) indicate continuous covariance after approximately 1500 A.D. at scales of 5-7 years. Coherency at sunspot-relevant scales is also present to a limited extent in each proxy, with significant peaks occurring sporadically throughout the LOI and MS records.

Figure 8 illustrates time series and WSP results over the period of record of the winter SOI reconstruction (1706-1977 A.D.), while wavelet coherency results between the SOI and Charco Verde a) charcoal, b) LOI, and c) MS are depicted in Figure 9. The dominant periodicity band within the SOI ranges from 3-4 years, yet prominent power peaks are also evident between 2-3 years, 6-9 years, and 11 yrs. Wavelet coherency results reveal limited significant covariance between the Charco Verde proxies and winter SOI. This could be largely due to limitations in the frequency resolution of the proxy records, which are limited to ~6 yrs on average while dominant SOI variability occurs every 3-4 years.

Comparison to Solar Activity Reconstructions

Figure 10 illustrates the $\Delta^{14}\text{C}$ time series data over the period analyzed and corresponding WSP results; Table 3 summarizes wavelet power peaks. High wavelet power is evident at scales of sunspot variability (11 and 22 years) throughout the record. Wavelet coherency analyses between the radiocarbon record and the charcoal, LOI, and MS proxies (Figs. 11a-c, Table 4) reveal statistically significant peaks at two primary periodicity bands: 3-7 years and 10-12 years, thus demonstrating covariance at frequencies of both ENSO and solar activity. Particularly noteworthy are coherency peaks after ~1500 A.D., which correlate to the Quelcayya - charcoal results (Fig. 7a). The $\Delta^{14}\text{C}$ - charcoal covariance plot (Fig. 11a) indicates additional peaks of significance at 1200-1300 A.D. and 900-950 A.D. at scales of 3-5 and 10-12 years, respectively, while the $\Delta^{14}\text{C}$ - LOI results (Fig. 10b) suggest significant covariance at ENSO-relevant scales

between 1300-1350, 1200-1250, and 800-850 A.D. By contrast, the $\Delta^{14}\text{C}$ - MS plot (Fig. 10c) indicates relatively consistent covariance at sunspot-relevant scales of 10-14 years prior to ~1200 A.D., with limited ENSO-scale coherency. These results suggest a possible relationship between fire regimes and droughts induced by fluctuations in solar activity, where the effects of biomass burning are also evident in the sediment organic content and erosion proxies.

Figure 12 illustrates time series and WSP results over the period of record of the group sunspot number (SN) reconstruction (1610-1995 A.D.), while wavelet coherency results between SN and Charco Verde a) charcoal, b) LOI, and c) MS are depicted in Figure 13. The sunspot data reveal an expectedly strong wavelet power band at ~11 years throughout the record, with the exception of periods sustained reductions in sunspot numbers and solar energy output (e.g., the Maunder Minimum at 1650-1720 A.D.). The strongest wavelet power peak occurs in the past 50 years, when sunspot activity and solar energy output is known to be relatively high. Wavelet coherency results between SN and the Charco Verde proxies do not indicate periods of sustained covariance. Sporadic coherency peaks significant at the 95% confidence level are present, however, particularly at 1820-1850 in the SN – charcoal plot (Fig. 13a). The SN – magnetic susceptibility plot additionally illustrates significant covariance between 1780-1800 A.D. at a scale of 6-7 years, and 1960-1975 at a scale of 7-10 years (Fig. 13c).

Chapter 4: Discussion, Conclusions, and Implications

DISCUSSION

Sources of Macroscopic Charcoal Fluctuations

In addition wildfire frequency, temporal fluctuations in the charcoal proxy may reflect changes in the erosional and depositional processes that transport charcoal material and/or changes in fuel load (Whitlock and Larsen, 2001). The charcoal record must therefore be compared to other paleoenvironmental proxies that may provide insight into whether charcoal variations are due to changes in fire frequencies or to auxiliary factors. Magnetic susceptibility (MS) and loss on ignition (LOI) data provide evidence of erosional activity and fuel accumulation, respectively, where high values in both records may suggest a natural cause of augmented charcoal concentration. As evident in Figs. 3c-d, the MS and LOI records are not well correlated to charcoal concentrations. If charcoal accumulation at Charco Verde was primarily a function of erosion rates as opposed to an overall escalation in burning activity, the charcoal and MS records would be expected to co-vary. Similarly, if a rise in charcoal-producing biomass generated elevated charcoal values, peaks in the LOI record would correspond to higher charcoal concentrations. Notably, these correlations do not occur in the Charco Verde sediments. From 581-950 A.D., magnetic susceptibility exhibits a variable, yet increasing trend while charcoal concentrations, although elevated, generally decline. Additionally, MS rapidly decreases and retains low values after 950 A.D., where charcoal concentrations increase to their maximum values and remain elevated until ~1300 A.D. The LOI record demonstrates relatively low organic content at depths of prominent charcoal peaks, with highest values occurring at 1750-1850 A.D. where charcoal values are at their nadir. High LOI levels at 1000-1200 A.D., indicating increased vegetation cover and more

charcoal production, may be partially responsible for the coeval charcoal climax; however, LOI rapidly declines at 1100 A.D. when charcoal reaches its zenith. The LOI record thus suggests that natural changes in vegetation abundance alone cannot produce the variations in charcoal concentrations. The lack of correlation between both MS and LOI reconstructions with the charcoal record largely discounts fuel load or erosion as the primary control of charcoal variations, thereby implicating anthropogenic or natural burning as the principal cause of charcoal fluctuations on Ometepe Island.

Significance of Proxy Record Covariance

Wavelet coherency results must be understood in the context of correlation analyses between drastically different proxy records, which respond to environmental forcing at different times and scales. In addition, the proxies themselves represent paleoenvironmental conditions of different scales: while the Charco Verde proxies record primarily watershed-level events, the Quelcayya ice core record documents local changes in snow accumulation in the Peruvian Andes—this region of the world may also experience a different response to ENSO forcing than that of lower Nicaragua. The $\Delta^{14}\text{C}$ reconstruction records hemispheric changes in atmospheric radiocarbon isotopic composition, while the SOI and sunspot records are globally averaged and reconstructed indices. Thus, although two records may be driven by the same climate mechanism, local auxiliary factors that also contribute to proxy fluctuations may obfuscate the primary forcing signal. Furthermore, the relationships between regional climate variability and local fire regimes are likely better approximated by a non-linear function; the attempt to measure linear covariance between such time series may therefore lead to erroneously low statistical significances. Despite these difficulties, the existing significant wavelet coherency peaks between the Charco Verde proxies and the long-term ENSO and sunspot

proxies reveal results that provide evidence of global climate forcing of local environmental conditions.

Periods of high coherency in wavelet covariance analyses isolate times within the records that respond to the same forcing mechanism—natural or anthropogenic—at the same scales. Particularly notable are the covariances between each Charco Verde proxy at 1) 581-700 A.D., 2) 850-900 A.D., 3) 1025-1150 A.D., and 4) 1300-1350 A.D., which correspond with four significant periods in the charcoal time series record: 1) a period of high initial charcoal values and variability; 2) a period of sustained, diminished charcoal values (the lowest pre-Conquest charcoal concentrations); 3) the record's peak charcoal values; and 4) the period of most rapid and severe charcoal decline. When considered with the charcoal WSP results, where significant power is notably absent between ~1000-1500 A.D. at the period of greatest overall time series variability, the charcoal record appears to record three phases of natural versus anthropogenic dominance: a period of combined anthropogenic and climatic influence from 581 A.D. becomes dominated by anthropogenic activity at 1000 A.D., which finally transitions into a naturally-forced record at ~1500 A.D. Covariance between the Charco Verde proxies before 1000 A.D. and after ~1500 A.D. is thus likely due to natural forcing, while that in between these two periods may be attributed to anthropogenic modification of the landscape.

The strong wavelet power at scales of ~7, 14, and 24 years in the charcoal record after ~1500 A.D. may therefore be indicative of the natural fire regime within the Ometepe tropical dry forests, which becomes prominent when the anthropogenic burning signal is diminished. With contiguous wavelet power significant at the 95% confidence level (Fig. 4a), the lack of coherency between the charcoal proxy and the short-term climate records (SOI and SN) (Figs. 9 and 13) does not preclude climate forcing. By contrast, low coherency may be due to the different response times of fire regimes to

changes in meteorological conditions, or to frequency resolution limitations in the charcoal record. This is particularly evident in Figs. 14 and 15, which illustrate the respective wavelet power spectra for the Charco Verde proxies between 1706-1977 and 1610-1995, the time periods of record of the SOI and sunspot indicators. Statistically significant fire cycles at 6-8 and 11-22 years over the entire 250 and 400 year periods (Figs. 14b and 15b, respectively) suggest possible climate forcing of fire frequencies, where lack of wavelet coherency may be due to the slightly different scales of dominant variability in the SOI (~3-4 years; Fig. 14a) and SN (~11 years; Fig. 15a) records. The fire regime within the tropical dry forests of Ometepe Island may thus be influenced by droughts induced by ENSO and/or fluctuations in solar energy output, with scales of response that are not precisely correlated with the scales of climatic variation. Prominent wavelet power at scales of 11 and 22 years is also present in the LOI record from 1700-1850 (Figs. 14c, 15c), as well as at 11 and 22 years throughout the period 1610-1995 in the magnetic susceptibility record (Fig. 15d). This contiguous and significant wavelet power at scales of sunspot variability may provide additional evidence of drought cycles on Ometepe Island, where erosion rates exhibit a more direct response to the local hydrologic balance than biomass burning.

Summary of Natural versus Anthropogenic Sources of Environmental Change on Ometepe Island

Early to middle San Roque Phase (581-800 A.D.)

The analysis of the Charco Verde environmental proxies in conjunction with archeological surveys provides insight into the relationship between ancient Ometepe societies and their environment. Nine cultural phases identified by Haberland (1986) are present during the time period of record, beginning with the San Roque Phase. High

charcoal concentrations, low sediment organic content, and high magnetic susceptibility values during this phase (Figs. 4a-c) suggests that the Ometepe population actively burned their landscape for agricultural and other purposes, decreasing natural vegetation abundance and increasing regional erosion rates. These findings corroborate the archeological description of the San Roque Phase as the pinnacle of cultural development on Ometepe Island. Despite the prevalence of anthropogenic burning, evidence of strong climate forcing potentially caused by variations in solar activity is additionally present: 1) a prominent wavelet power peak in the charcoal record between 590-750 A.D. at a scale of ~22-32 years; 2) Charco Verde proxy record coherence between 581-700 A.D.; and 3) significant coherence between the Charco Verde proxies and the $\Delta^{14}\text{C}$ record between 581-600 A.D. (Fig. 4a, Table 3). This contention is supported by Quelcayya ice core time series data, which demonstrate the occurrence of a severe, 32-year drought in the late 6th century followed by a 40-year period of increased precipitation, in turn followed by dry conditions (Thompson et al., 1985).

San Roque - Gato Phase Transition (750 - 950 A.D.)

Although charcoal concentrations steadily decline through the late San Roque Phase and may suggest that a period of increased precipitation curtailed fire frequencies, wet conditions are not consistent with the Charco Verde proxies: high erosion rates combined with extremely low sediment organic content are not representative of a wet environment. Rather than a consequence of a higher precipitation, declining charcoal concentrations at 750-950 A.D. may be caused by reduced anthropogenic burning due to the onset of drought, in turn leading to a reduction in Ometepe Island's agricultural capacity. Hodell et al. (1995, 2001, 2005) suggest that the period 800-1000 A.D. was the driest of the middle to late Holocene in the Yucatan Peninsula, a drought that may have contributed to the collapse of the Classic Maya and surrounding populations. Ancient

Puebloan Mesa Verde reservoirs in Colorado (Van West, 1991), multiple paleoclimate records from California (Schimmelmann, 2003), and reduced snow accumulation at Quelcayya (Thompson et al., 1985; Fig. 6) additionally indicate drought cycles between 800-1000 A.D., thus demonstrating the severity and extent of dry conditions through this period. Evidence of similar, coeval climate events in the Charco Verde proxies include: 1) peak wavelet power at scales of 2-5, 5-8, and 10-15 years between 750-1000 A.D. (Fig. 4a, Table 3); 2) charcoal, LOI, and MS record covariance between 850-900 A.D. at scales of 2-11 years. (Fig. 5, Table 4); and 3) Quelcayya - charcoal and $\Delta^{14}\text{C}$ - charcoal covariance at scales of 2-7 and 10-12 years between 800-1000 A.D. (Figs. 7a and 11a, Table 4). When analyzed in conjunction with declining charcoal concentrations, high erosion rates, and the lowest organic content values of record, these results provide evidence of Ometepe Island indigenous community response to widespread and prolonged drought caused by short-term climate variability, where burning declined because of reduced agricultural activities and/or total island population.

Gato Phase (950-1200 A.D.)

The Gato Phase of Ometepe cultural development beginning between 900-950 A.D. is delineated by new ceramic traditions that suggest an influx of settlers to the island and a recovery of island populations. Charcoal concentrations begin to rise precisely at the onset of this phase and steadily increase to their zenith, suggesting greater indigenous burning activities. However, correspondence of peak charcoal concentrations with multiple regional climate records indicating sporadic drought conditions between 1130-1180 A.D. (Van West, 1991; Hodell, 2005) and 1240-1300 A.D. (Thompson et al., 1985; Van West, 1991) suggest that although the charcoal signal may be dominated by anthropogenic burning (e.g., no wavelet power peaks), dry conditions continued to affect local fire regimes. These regional dry periods additionally correspond with significant

peaks in the $\Delta^{14}\text{C}$ - charcoal wavelet coherency results at 2-7 years, as well as peaks in the Quelcayya - charcoal coherency at sunspot-relevant scales (Figs. 7a and 11a, Table 4). Despite the absence of significant wavelet power in the charcoal record, ENSO and/or fluctuations in solar activity thus appear to have continued to influence the fire regime on Ometepe Island during the Gato Phase.

La Paloma and San Lazaro Phases (1200-1400 A.D.)

Charcoal concentrations experience their most rapid decline during the transition between the La Paloma and San Lazaro Phases at 1300 A.D., and remain relatively low during the latter period of cultural development. Archeological data indicate that Lake Nicaragua water levels during the San Lazaro fluctuated significantly, and evidence of climate forcing is demonstrated by wavelet power between 1300-1400 A.D. centered on a scale of 10-20 years in the LOI record.

Santa Ana Phase (1400-1550 A.D.) and European Contact

The Santa Ana phase, or the final pre-Conquest phase of cultural development on Ometepe Island, is again characterized by an influx of indigenous migrants by archeological surveys. However, decreased charcoal concentrations combined with high wavelet power at ENSO- and sunspot-relevant scales suggest the transition to a naturally-dominated proxy record that becomes primarily reflective of climate forcing after Spanish arrival (~1522 A.D.). Coherency results between the charcoal and Quelcayya records demonstrate peak covariance at ENSO frequencies that appear precisely at the time of European contact, remaining contiguous through the length of the record (Fig. 7a). Coherency peaks between the $\Delta^{14}\text{C}$ and Charco Verde proxies at both ENSO and sunspot scales additionally become continuous during this period, with results significant at the 95% confidence level (Fig. 11). The cessation of indigenous burning activities

upon European arrival is likely responsible for the sudden coherency increase between the proxy records (Suman, 1991), as the response of the Ometepe fire regime to ENSO and/or sunspot cycles is able to dominate fluctuations in the charcoal record at this time (Figs. 14, 15).

CONCLUSIONS

In this study, I examined the relationship between short-term climate variability, paleo-fires, and anthropogenic sources of environmental change over the past 1,400 years on Ometepe Island. Macroscopic charcoal, loss on ignition, and magnetic susceptibility records were reconstructed from the Charco Verde lake sediment core, and statistical wavelet analyses were performed to contextualize natural fire regimes in this under-investigated tropical biome. Wavelet analysis proved a successful means to extricate natural from anthropogenic sources of environmental change evidenced in paleoproxy data. Results from this project suggest that fire regimes on Ometepe Island respond to high frequency (sub-centennial scale) climate variations potentially due to the 11- and 22-year sunspot cycles and/or severe ENSO events, and support regional paleoenvironmental analyses by providing evidence of anthropogenic environmental impacts between ~600 and 1500 A.D. with a drastic decline after European contact. Possible evidence of widespread drought conditions between 800 - 1000 A.D. and 1150 – 1300 A.D. is additionally present in both the time series data and wavelet power spectra.

Specific results from this study include the following:

1. Wavelet transform analysis is an effective means to investigate sources of data fluctuations in paleoenvironmental proxies through identifying nonstationary signals that correspond to various climate mechanisms. Unlike Fourier analyses that assume constant frequencies throughout the period of analysis, wavelet transforms localize multiple

forcing mechanisms via their different frequency signatures. Prolonged periods of low wavelet power suggest the dominance of human activity on proxy data variations, while high wavelet power is indicative of climate forcing. Wavelet power and coherency peaks were most evident after preprocessing by a 2-32 year bandpass filter of log-transformed data.

2. Wavelet results suggest natural fire cycles at scales of ~7, 14, and 24 years in the tropical dry forests of Ometepe Island. These periodicities are particularly evident when charcoal fluctuations are analyzed within the post-Contact timeframe (e.g., after ~1500 A.D.; Figs. 14, 15). The natural fire regime of Ometepe Island may thus be influenced by climate mechanisms at interannual and decadal scales.

3. Wavelet analysis of the Charco Verde proxies indicate that fire regimes and environmental change initially dominated by a mixed climatic-anthropogenic signal transitioned to that dominated by anthropogenic environmental impacts—especially increased burning activity—at ~1000 A.D. Anthropogenic dominance persisted until ~1500 A.D. when the arrival of Europeans likely decimated indigenous populations, thus reducing biomass burning and other land use activities. These results are supported by preliminary pollen data from the Charco Verde core, as well as by similar finding in regional paleoecological studies.

4. Wavelet coherency analyses identify periods of covariance between two time series at various scales, thus suggesting a common forcing mechanism—natural or anthropogenic—in driving data changes. Results between the Charco Verde and the regional climate proxies (Quelcayya and $\Delta^{14}\text{C}$) indicate periods of covariance throughout the record, particularly after European contact at ~1500 A.D. High coherency with both the Quelcayya and $\Delta^{14}\text{C}$ record post-European contact is likely a function of natural dominance of the proxy signals once anthropogenic impacts were diminished, thus

revealing the effect of ENSO events and solar cycles on fire regimes. Although the Quelcayya, SOI, and SN coherency peaks are not always statistically significant at the 95% confidence level, these results remain important when considered in conjunction with the different lag times and distinct response magnitudes that obfuscate proxy record covariance—even when forced by the same climate mechanism.

5. Although wavelet power in the Charco Verde proxies is low through the period 1500-1000 A.D., evidence of climate forcing of fire regimes—where the climate cycles are likely obscured by frequent anthropogenic burning—exists in the charcoal and LOI records. Temporal correlation between peak charcoal concentrations and regional climate proxies indicating coeval droughts in the southwestern U.S. and northern South America occur between 1130-1180 A.D. and 1240-1300 A.D (Thompson et al., 1985; Hodell et al., 2001; Van Buren, 2001; Schimmelmänn et al., 2003). A peak in LOI wavelet power from 1300-1400 A.D. at scales of 2-32 years corresponding with archeological records of fluctuating water levels in Lake Nicaragua provides additional evidence of natural sources of environmental change during this time.

6. Significant wavelet power prior to ~1000 A.D. is likely due to particularly strong climate forcing that manifests itself against a backdrop of anthropogenic activity. This finding is supported by regional investigations identifying the periods 550-590 A.D. and 800-1000 A.D. as especially dry, where the latter dry spell may have contributed to the collapse of the Maya and other civilizations due to severe water deficits (Hodell et al., 1995; Hodell et al., 2001; Van Buren, 2001; Schimmelmänn et al., 2003; Haug et al., 2003). A steady reduction in charcoal concentrations, an increase in erosion rates, and extremely low sediment organic content through this period may indicate that Ometepe indigenous communities were also affected by drought conditions, which severely curtailed their agricultural capacity. When considered with wavelet power and coherency

results from the Charco Verde and regional climate proxies, this study suggests that climate forcing of regional drought has occurred on sub-centennial timescales on Ometepe Island, thus invoking ENSO and/or high frequency variations in solar activity as a potential source.

IMPLICATIONS

The charcoal record suggests that fire frequencies on Ometepe Island decreased through the San Roque Phase, reaching a pre-Conquest minimum at ~900 A.D. and subsequently rising through the Gato Phase, with peak values occurring at ~1150 A.D. Charcoal concentrations then decline almost an order of magnitude through the La Poloma and San Lazaro phases (1200-1400 A.D.), with low fire frequencies during the island's post-Contact history. These results indicate that contemporary burning in the tropical dry forests of Ometepe Island is almost an order of magnitude lower than during the peak of indigenous community cultural development (Haberland, 1986). Environmental disturbance on the island also appears to have primarily occurred through the San Roque Phase (~600-1000 A.D.), with high magnetic susceptibility and low loss on ignition values indicating increased rates of erosion on a landscape with less natural vegetation. This analysis is supported by preliminary pollen work from the Charco Verde lake sediment core, where abundant maize (*Zea*), weed (*Asteraceae*), and grass (*Poaceae*) pollen suggest a highly disturbed landscape due to agriculture during this time; weed and grass pollen are subsequently replaced by lowland tropical tree species (*Ficus* and *Urticales*) after ~1500 A.D.

Suman (1991) similarly documented a decrease in charcoal concentrations and landscape disturbance in Nicaragua after ~1500 A.D., attributing this phenomenon to an essential cessation of burning activities when European contact decimated local

indigenous populations. Denevan (1961) suggests that the Nicaraguan native population was reduced to 5% of its pre-Conquest value—from ~600,000 to ~30,000 people—upon the arrival of the Spanish in 1522 A.D. The Spanish introduced cattle to Central America, and heavy grazing combined with indigenous population decline may account for decreased charcoal concentrations on Ometepe Island (Johannessen, 1963; Suman, 1991). Although populations in rural Central America have increased dramatically through the last two centuries (International Institute for Environment and Development, 1987), a lack of corresponding fire activity on Ometepe Island may be due to 1) modern production of export crops such as coffee, cotton, and bananas that do not require regular burning (Parker, 1964); and 2) livestock management techniques that do not heavily depend on the use of fire (Suman, 1991). Paleocological analyses of lake sediments in Guatemala, Costa Rica, and El Salvador additionally document similar environmental histories, with the highest concentrations of charcoal and disturbance pollen species occurring from 200-900 A.D. and decreased fire frequencies and environmental disturbance post-European contact (Tsukada and Deevey, 1967; Brenner et al., 1990; Dull, 2004a, Dull, 2004b; Anchukaitis and Horn, 2005).

The successful application of wavelets to the paleoproxy records used in this study (macroscopic charcoal, loss on ignition, and magnetic susceptibility) provides a new methodology for the analysis of historical environmental records that have both natural and anthropogenic contributions. Wavelet results of the charcoal reconstruction indicate natural fire cycles at ~7, 14, and 24 years that may be attributable to short term climate forcing, particularly ENSO events and/or fluctuations in solar activity on decadal scales. Unfortunately, the resolution of the charcoal record precluded analysis at scales less than 6 years on average; with higher resolution, ENSO covariance measures may have been stronger as evident by the dominant ~4-year frequency in both the SOI (Fig.

14a) and Quelcayya (Fig. 7) records. Despite the lack of statistical covariance with the ENSO reconstructions, the strong wavelet power at climate-relevant scales in the charcoal record—particularly after anthropogenic activity is diminished at ~1500 A.D. (Figs. 14 and 15)—is suggestive of a natural fire regime in Ometepe’s tropical dry forest that responds to short term climate variability.

The results of this study will contribute to the scientific community’s understanding of the dynamics of TDF fire regimes, and will help improve forest management and preservation initiatives on Ometepe Island and southwestern Nicaragua. These results will be bolstered by future work from the Charco Verde lake sediment core that is currently underway, including the reconstruction of high resolution pollen samples and stable carbon isotopes $\delta^{13}\text{C}$ in order to document changes in vegetation and lake levels over the past 1,400 years. Additionally underway is a large-scale coring initiative within Lake Nicaragua, where these paleoecological records will be compared to those of Charco Verde in both time and frequency space in order to provide robust evidence of tropical dry forest fire regimes, short term climate variability, and environmental change in southwestern Nicaragua on a *regional* scale. A lake sediment core from the top of Volcan Maderas on Ometepe Island (Fig. 1) has additionally been analyzed for charcoal, loss on ignition, and magnetic susceptibility; however, chronology issues within this core must be rectified before comparisons can be made to the Charco Verde records.

Table 1: Cultural history of indigenous communities on Ometepe Island from 2000 B.C.

Cultural Phase	Duration	Settlement and Subsistence Activities
Dinarte Phase	2000 – 500 B.C.	Farming, hunting, fishing on Volcan Concepción; no evidence of maize agriculture
Angeles Phase	500 – 200 B.C.	Same activities as above; phases separated due to volcanic eruption
Sinacapa Phase	200 B.C – 1 A.D.	Earliest record of settlement of Volcan Maderas, increased island population, and maize cultivation
Mantiel Phase	1 – 500 A.D.	Evidence of continued farming, hunting, fishing; increased volcanic activity leads to partial abandonment of Ometepe
San Roque Phase	500 – 950 A.D.	Evidence of increased maize agriculture and hunting, introduction of primal burials; pinnacle of cultural development on Ometepe Island, correspondence with Greater Nicoya development
Gato Phase	1000 – 1200 A.D.	New ceramic traditions indicate influx of settlers
La Paloma Phase	1200 – 1300 A.D.	Same ceramic tradition as above
San Lazaro Phase	1300 – 1400 A.D.	Significant fluctuation in Lake Nicaragua water levels
Santa Ana Phase	1400 – 1550 A.D.	Last pre-Conquest phase of indigenous activities; new ceramic traditions indicate influx of immigrants from Atlantic coast of lower Central America
Post-Spanish Contact	1550 A.D. – Present	Indigenous population decline; clashes between local populations and European settlers; current economy based upon tourism, livestock, and agriculture

Table 2: Radiocarbon sampling and age calibration results.

Sample ID	Depth (cm)	UCIAMS Number	Age - Median Probability \pm Error (^{14}C Years B.P.)	Lower - Upper 1σ Range (Years A.D.)	Lower - Upper 2σ Range (Years A.D.)	Calibrated Age - Median Probability (Years A.D.)
Charco Verde 314	314	32318	705 \pm 25	1274 - 1292	1264 - 1301	1284
Charco Verde 372	372	11792	865 \pm 25	1163 - 1212	1151 - 1225	1183
Charco Verde 421	421	32319	1010 \pm 15	1013 - 1027	993 - 1030	1018
Charco Verde 498	498	11793	1190 \pm 20	811 - 848	777 - 888	835
Charco Verde 586	586	11794	1230 \pm 20	788 - 819	765 - 876	789
Charco Verde 622	622	32320	1420 \pm 15	622 - 648	606 - 653	633

Table 3: Summary of time and scale of wavelet power maxima in proxy records analyzed.

Proxy Record	Time Period of Peak Wavelet Power (Years A.D.)	Scale of Peak Wavelet Power (Years)
Charco Verde Macroscopic Charcoal	1500 - 2004	2-8, 10-17, 21-28
	800 - 1000	10-14
	750 - 850	2-8
	600 - 775	21-31
Charco Verde LOI	1940 - 1980	8-12
	1600 - 1800	8-13
	1300 - 1400	2-32 (highest power at 10-22)
	800 - 1000	11-16, 22-32
	750 - 850	2-10
	590 - 650	14-20
Charco Verde MS	1750 - 1850	10-13, 16-22
	850 - 1000	19-32
	750 - 850	2-32 (highest power at 6-11)
Quelcayya Ice Core Snow Accumulation	Throughout record	2-7
	1600 - 1700	18-28
	1300 - 1400	20-28
	900 - 1100	16-32
	775-850	21-28
$\Delta^{14}\text{C}$ (Northern Hemisphere)	800 - 2004	20-32
	1250 - 1350	15 - 22
	1600 - 2004	7 - 22

Table 4: Summary of time and scale of wavelet coherency maxima of proxy records analyzed.

Proxy Records	Time Period of Peak Wavelet Power (years A.D.)	Scale of Peak Wavelet Power (years)
Charco Verde Macroscopic Charcoal - LOI	1500 - 2004	2-7
	1750 - 1850	2-11, 18-22
	1300 - 1350	2-7
	1025 - 1150	2-6, 7-11
	850 - 900	2-7, 11
	581 - 700	2-7
Charco Verde Macroscopic Charcoal - MS	1900 - 1925	2-5
	1300 - 1350	2-7
	1025 - 1150	2-6, 7-11
	850 - 900	2-7, 11
	581 - 700	2-7
Charco Verde MS - LOI	1300 - 1350	2-7
	1025 - 1150	2-6, 7-11
	850 - 900	2-7, 11
	581 - 700	2-7
Quelcayya - Charco Verde Macroscopic Charcoal	1500 - 2004	2-3, 5-7
	1650 - 1750	10-12
	1200 - 1350	6-8, 10-22
	900 - 1000	5-7
	850 - 900	10-22
$\Delta^{14}\text{C}$ - Charco Verde Macroscopic Charcoal	1500 - 2004	5-7, 7-12
	1200 - 1300	2-4, 10-13
	900 - 950	10-12
	590 - 600	2-7



Figure 1: Site map depicting Ometepe Island and Laguna Charco Verde within southwestern Nicaragua. Laguna Charco Verde is located within a peninsula on the southern side of Volcan Concepción, marked by the filled black circle.

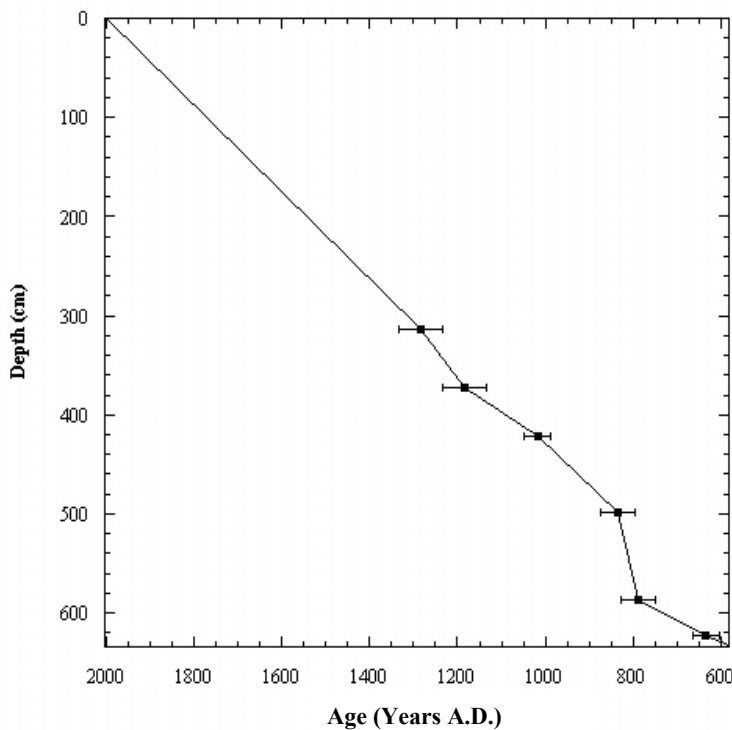


Figure 2: Depth-age (calibrated in years A.D.) relationship of the Charco Verde lake sediment core. Error bars mark the one-sigma median probability range.

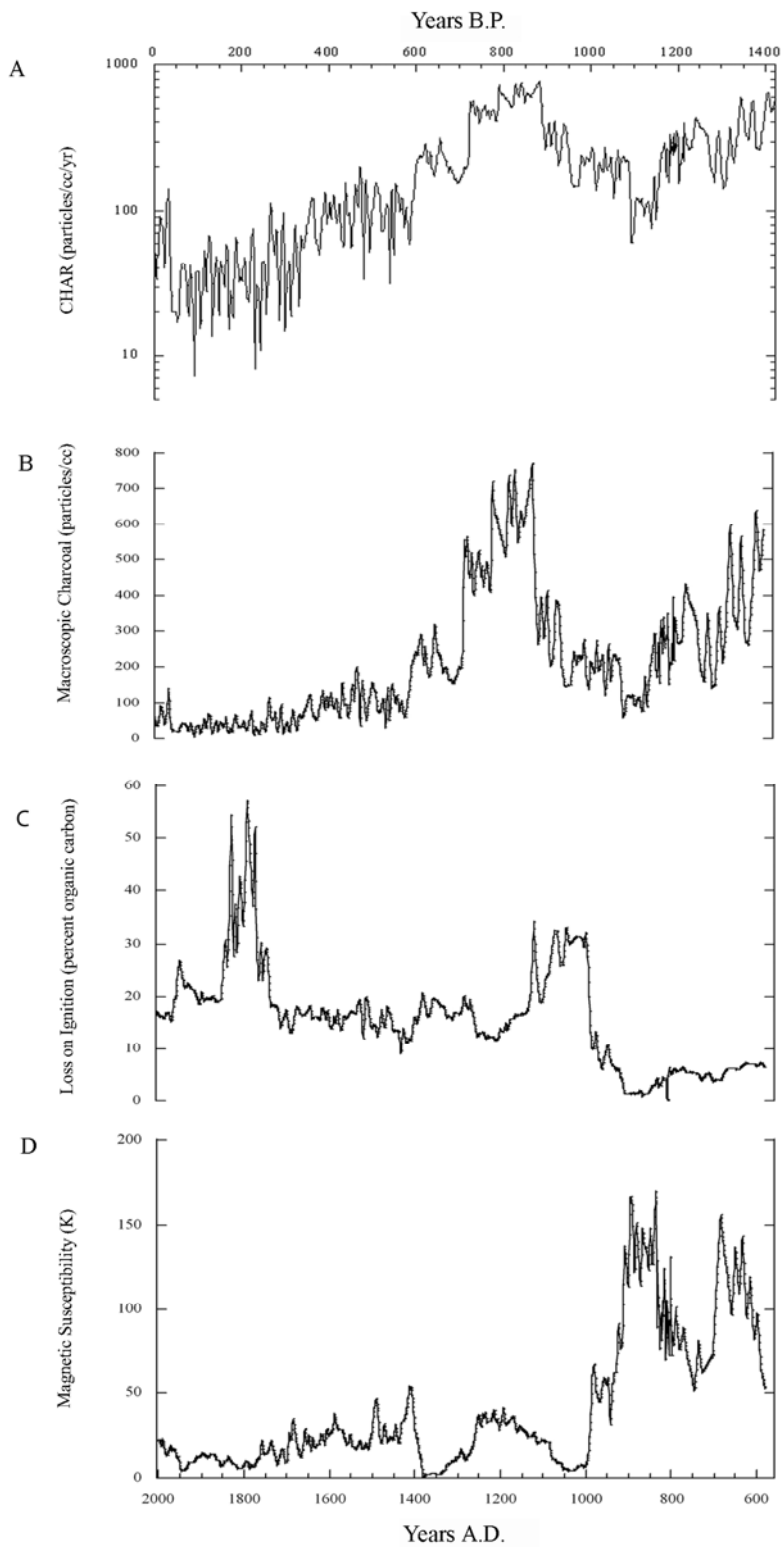


Figure 3: Time series results of the Charco Verde lake sediment core: A) charcoal accumulation rates (CHAR, note the log scale); B) macroscopic charcoal concentrations; C) loss on ignition; and D) magnetic susceptibility.

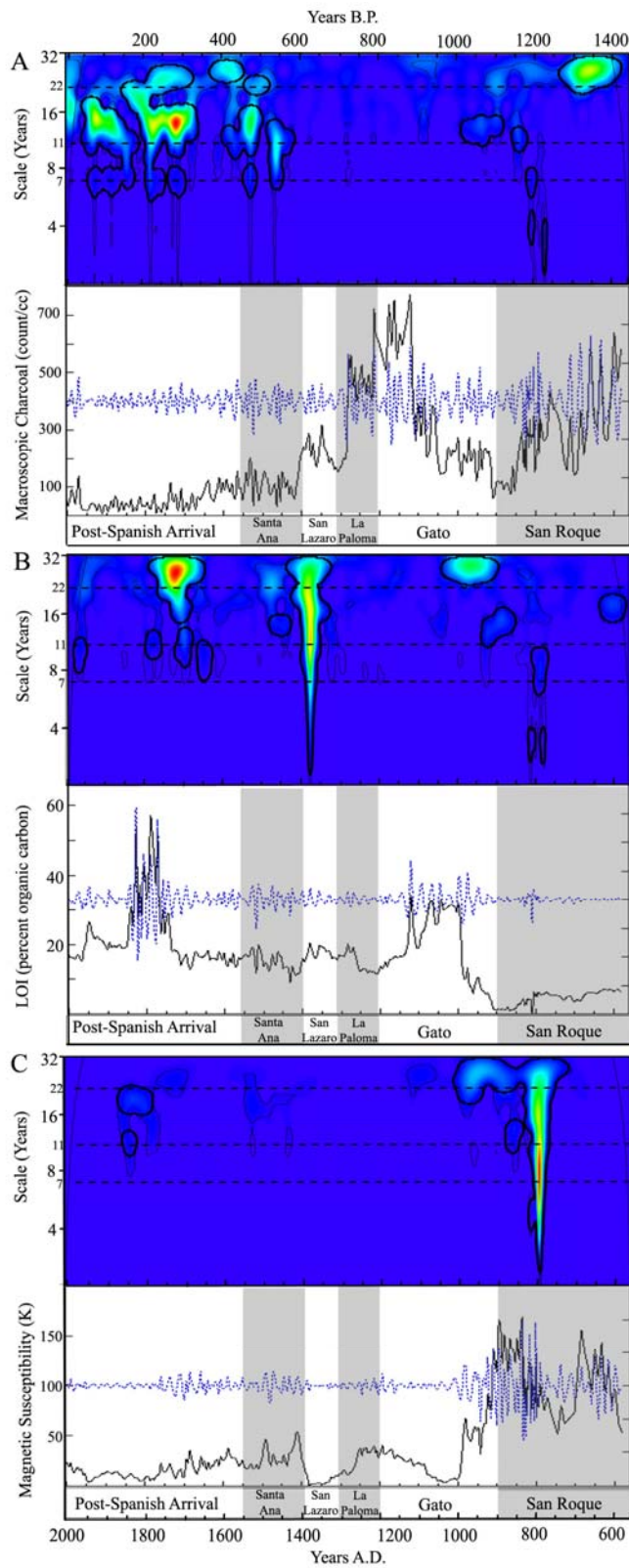


Figure 4: Wavelet power spectra (top) and time series (bottom) plots of the Charco Verde paleoproxies: A) macroscopic charcoal; B) loss on ignition; and C) magnetic susceptibility. Bandpass filtered series from 2-32 years (blue dashed line) of log-transformed data are plotted with the unfiltered time series data (black). Significant wavelet power peaks at the 95% confidence level are delineated by 1) point-wise (thin black lines) and 2) area-wise testing (thick black lines), where the latter significance test is considered more conservative (Maraun and Kurths, 2004).

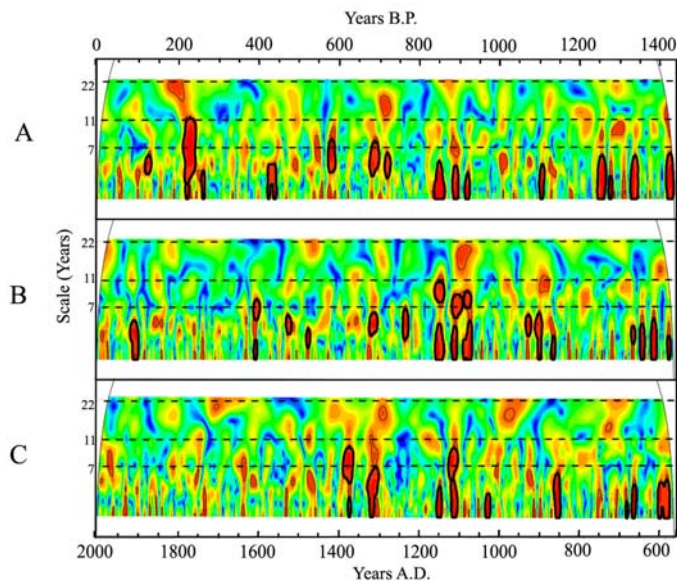


Figure 5: Wavelet coherency plots of the Charco Verde paleoproxies: A) macroscopic charcoal – loss on ignition; B) macroscopic charcoal – magnetic susceptibility; and C) magnetic susceptibility – loss on ignition. Significant wavelet power peaks at the 95% confidence level are delineated by 1) point-wise (thin black lines) and 2) area-wise testing (thick black lines), where the latter significance test is considered more conservative (Maraun and Kurths, 2004).

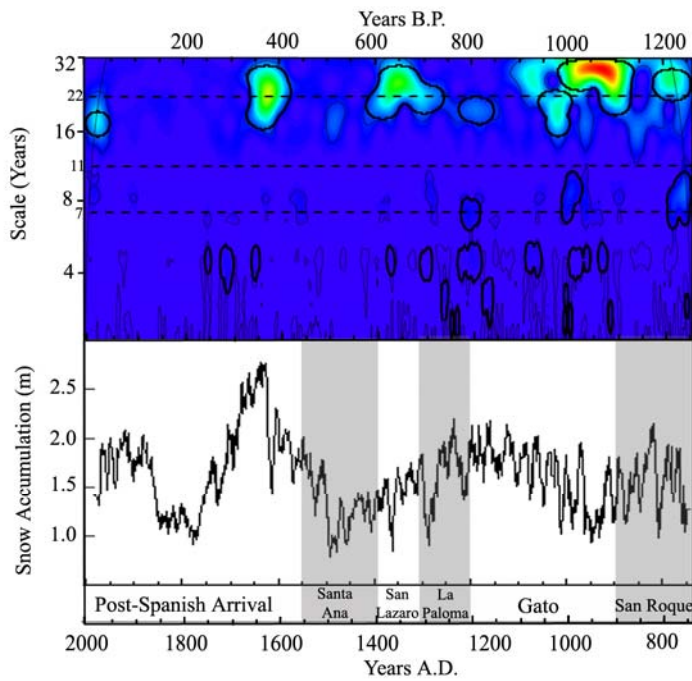


Figure 6: Wavelet power spectrum (top) and time series (bottom) plot of Quelcayya ice core snow accumulation (Thompson et al., 1984). Periods of low snow accumulation are indicative of regional drought. Significant wavelet power peaks at the 95% confidence level are delineated by 1) point-wise (thin black lines) and 2) area-wise testing (thick black lines), where the latter significance test is considered more conservative (Maraun and Kurths, 2004).

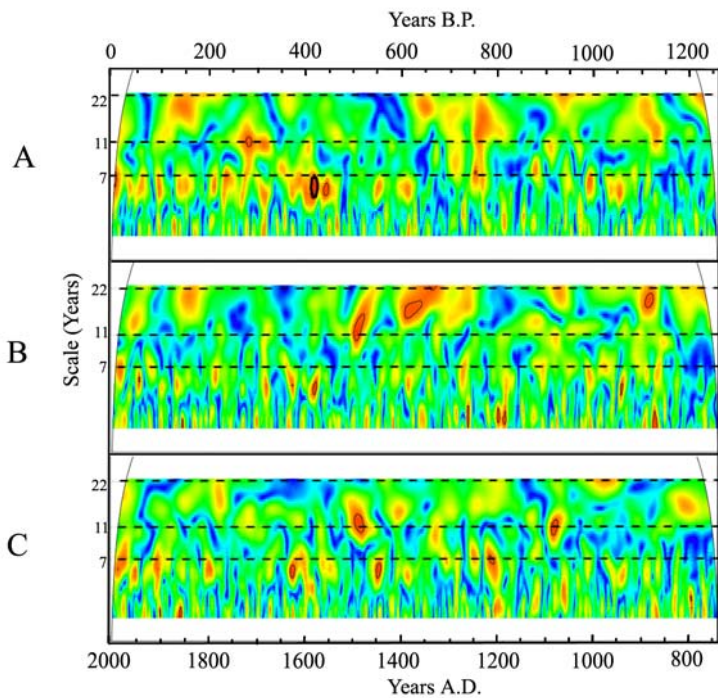


Figure 7: Wavelet coherency plots of Quelcayya ice core snow accumulation (Thompson et al., 1984) and Charco Verde proxies: A) Quelcayya – macroscopic charcoal; B) Quelcayya – loss on ignition; and C) Quelcayya – magnetic susceptibility. Significant wavelet power peaks at the 95% confidence level are delineated by 1) point-wise (thin black lines) and 2) area-wise testing (thick black lines), where the latter significance test is considered more conservative (Maraun and Kurths, 2004).

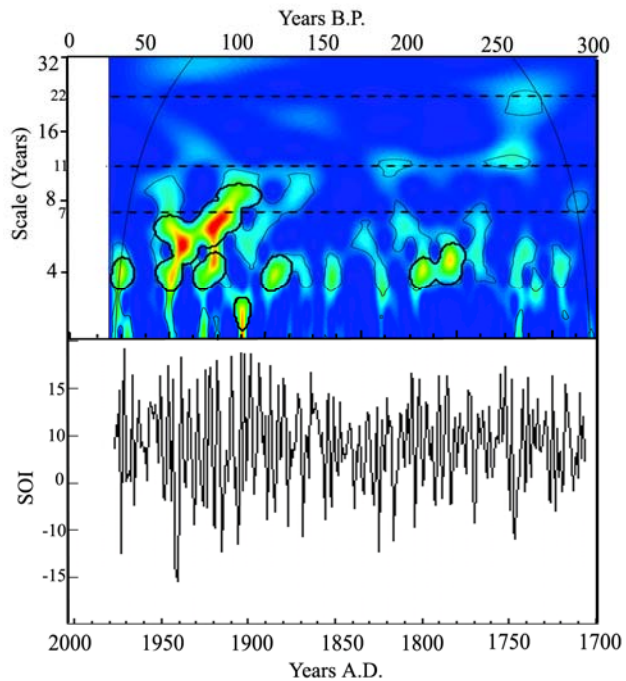


Figure 8: Wavelet power spectrum (top) and time series (bottom) plot of reconstructed winter SOI (Stahle et al., 1998). Negative excursions of the SOI indicate El Niño events. Significant wavelet power peaks at the 95% confidence level are delineated by 1) point-wise (thin black lines) and 2) area-wise testing (thick black lines), where the latter significance test is considered more conservative (Maraun and Kurths, 2004).

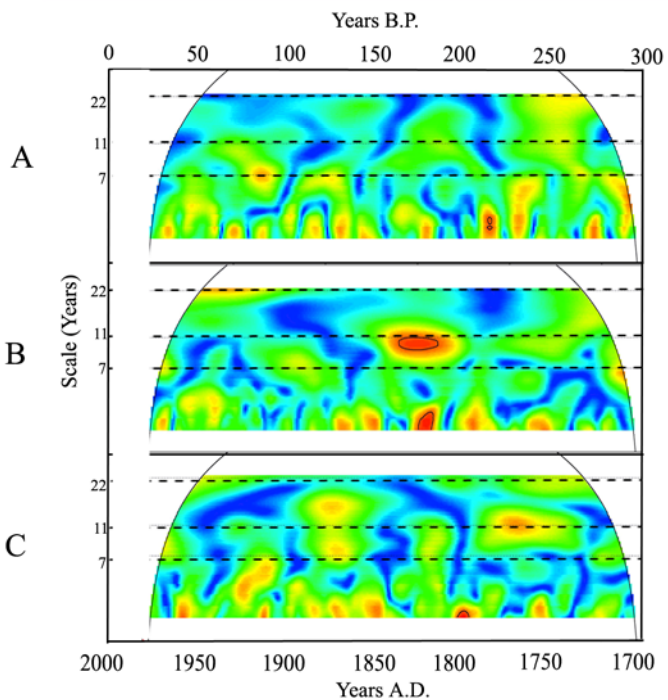


Figure 9: Wavelet coherency plots of reconstructed winter SOI (Stahle et al., 1998) and Charco Verde proxies: A) SOI – macroscopic charcoal; B) SOI – loss on ignition; and C) SOI – magnetic susceptibility. Significant wavelet power peaks at the 95% confidence level are delineated by 1) point-wise (thin black lines) and 2) area-wise testing (thick black lines), where the latter significance test is considered more conservative (Maraun and Kurths, 2004).

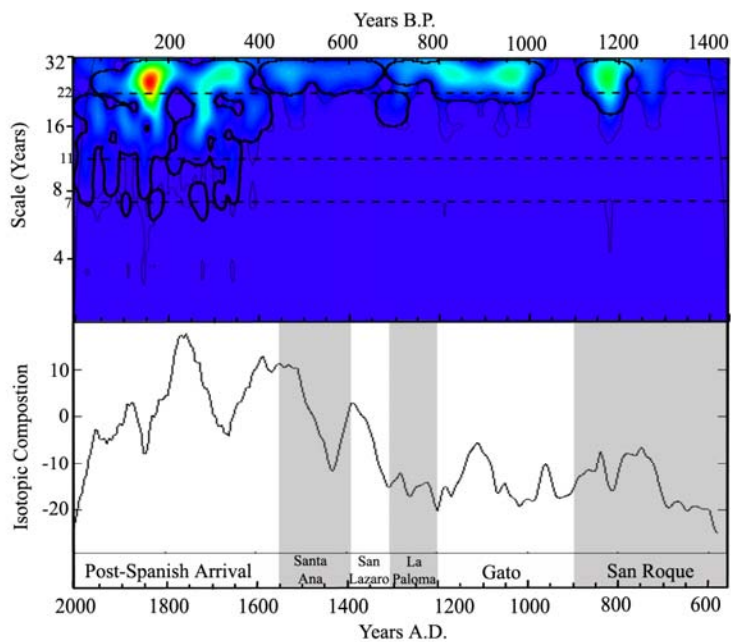


Figure 10: Wavelet power spectrum (top) and time series (bottom) plot of northern hemisphere radiocarbon ($\Delta^{14}\text{C}$) (Reimer et al., 2004). Periods of lighter isotopic composition suggest increased solar energy output. Significant wavelet power peaks at the 95% confidence level are delineated by 1) point-wise (thin black lines) and 2) area-wise testing (thick black lines), where the latter significance test is considered more conservative (Maraun and Kurths, 2004).

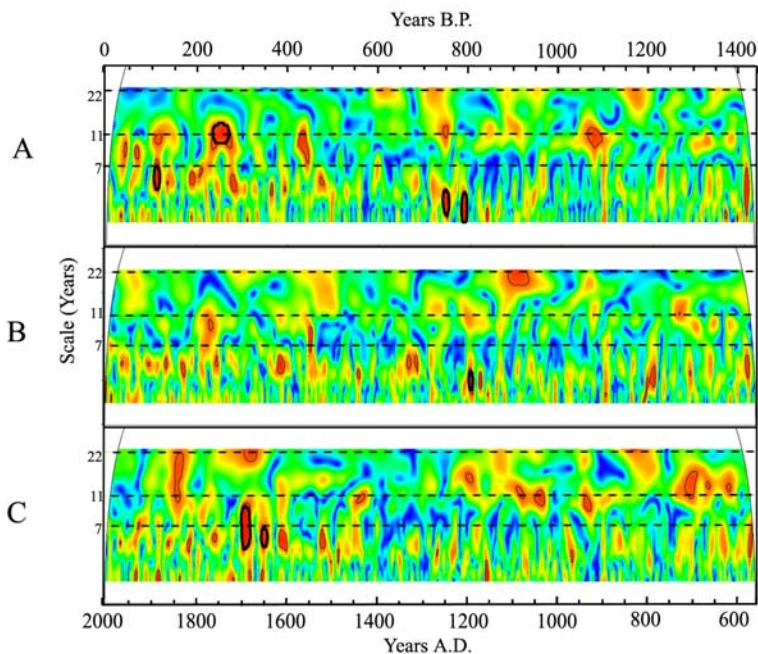


Figure 11: Wavelet coherency plots of northern hemisphere radiocarbon ($\Delta^{14}\text{C}$) (Reimer et al., 2004) and Charco Verde proxies: A) $\Delta^{14}\text{C}$ – macroscopic charcoal; B) $\Delta^{14}\text{C}$ – loss on ignition; and C) $\Delta^{14}\text{C}$ – magnetic susceptibility. Significant wavelet power peaks at the 95% confidence level are delineated by 1) point-wise (thin black lines) and 2) area-wise testing (thick black lines), where the latter significance test is considered more conservative (Maraun and Kurths, 2004).

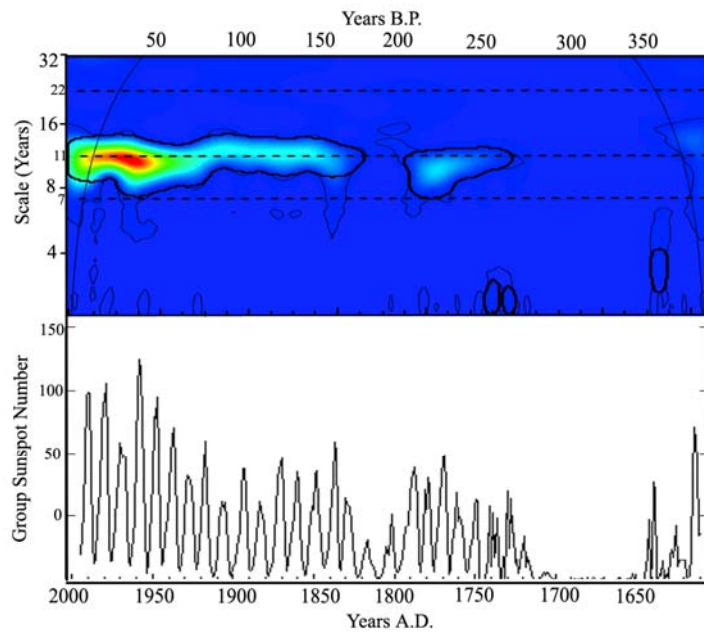


Figure 12: Wavelet power spectrum (top) and time series (bottom) plot of group sunspot number (Hoyt and Schatten, 1998). High sunspot numbers indicate greater solar energy output. Significant wavelet power peaks at the 95% confidence level are delineated by 1) point-wise (thin black lines) and 2) area-wise testing (thick black lines), where the latter significance test is considered more conservative (Maraun and Kurths, 2004).

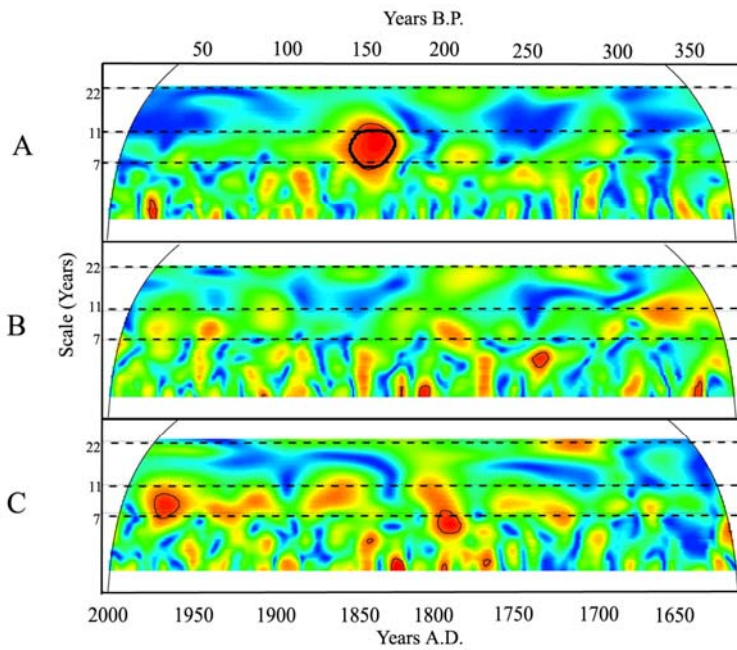


Figure 13: Wavelet coherence plots of group sunspot number (SN) (Hoyt and Schatten, 1998) and Charco Verde proxies: A) SN–macroscopic charcoal; B) SN – loss on ignition; and C) SN – magnetic susceptibility. Significant wavelet power peaks at the 95% confidence level are delineated by 1) point-wise (thin black lines) and 2) area-wise testing (thick black lines), where the latter significance test is considered more conservative (Maraun and Kurths, 2004).

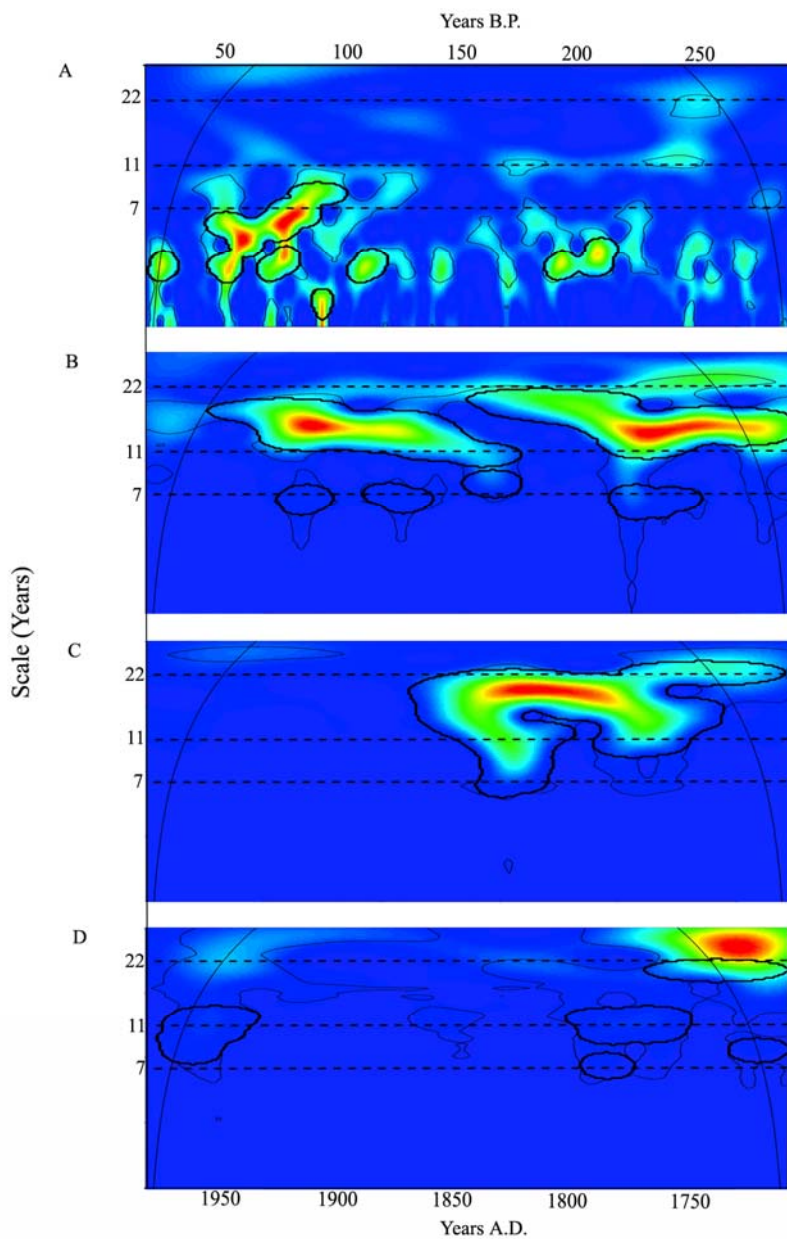


Figure 14: Wavelet power spectra over the time period 1706-1977 A.D. for A) reconstructed SOI (Stahle et al., 1998); B) macroscopic charcoal; C) loss on ignition; and D) magnetic susceptibility. Significant wavelet power peaks at the 95% confidence level are delineated by 1) point-wise (thin black lines) and 2) area-wise testing (thick black lines), where the latter significance test is considered more conservative (Maraun and Kurths, 2004).

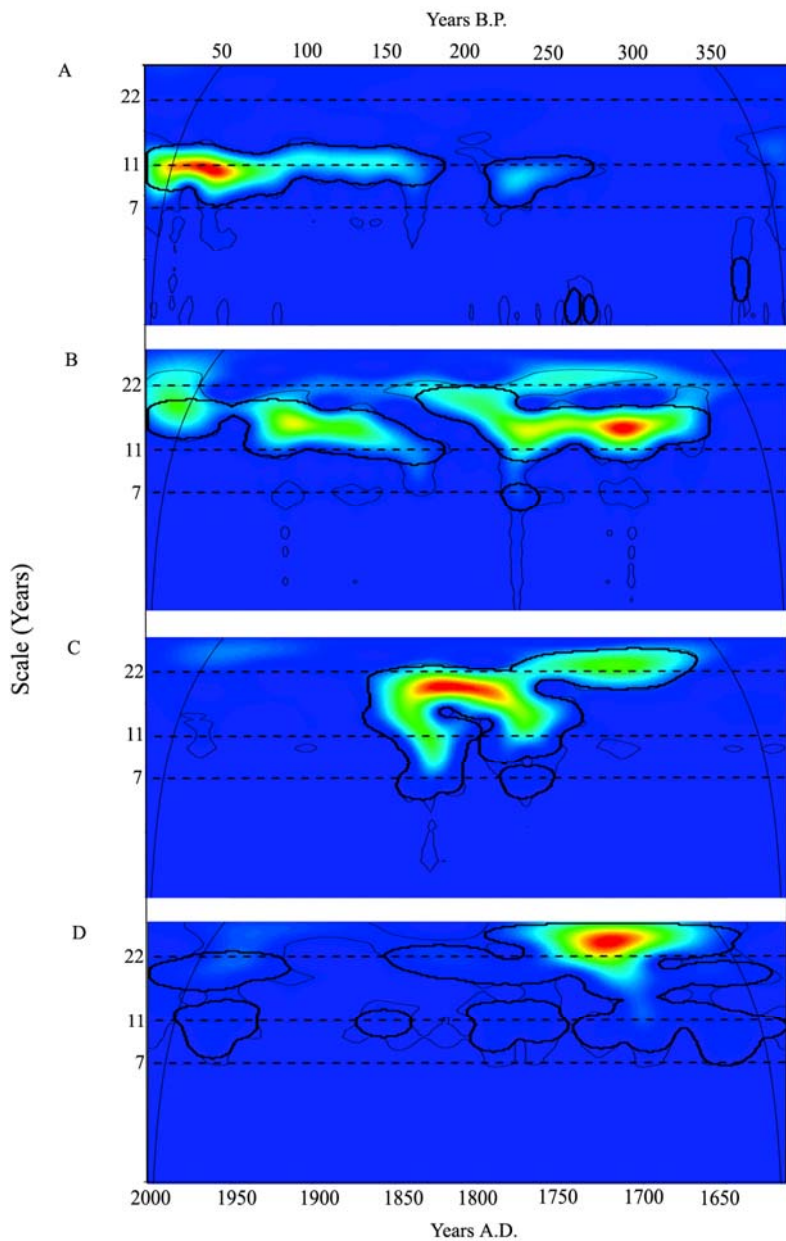
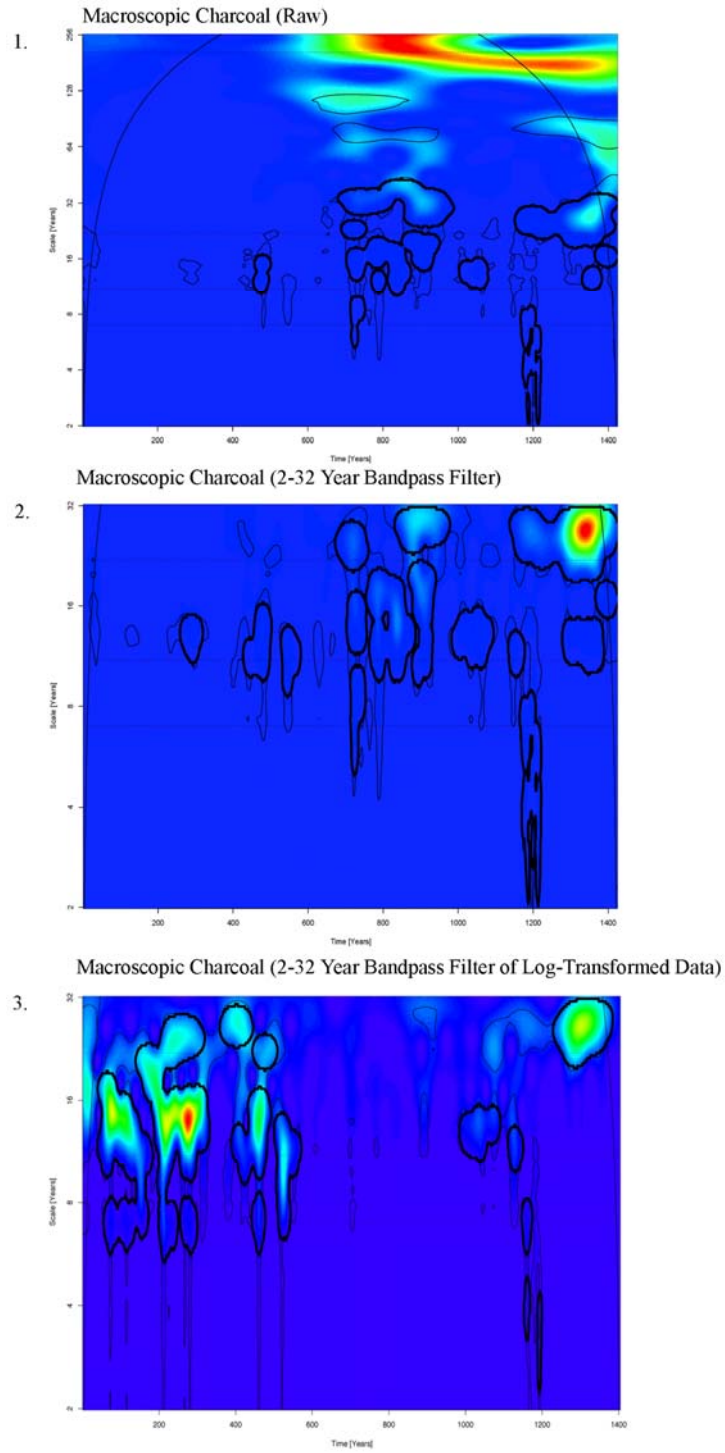
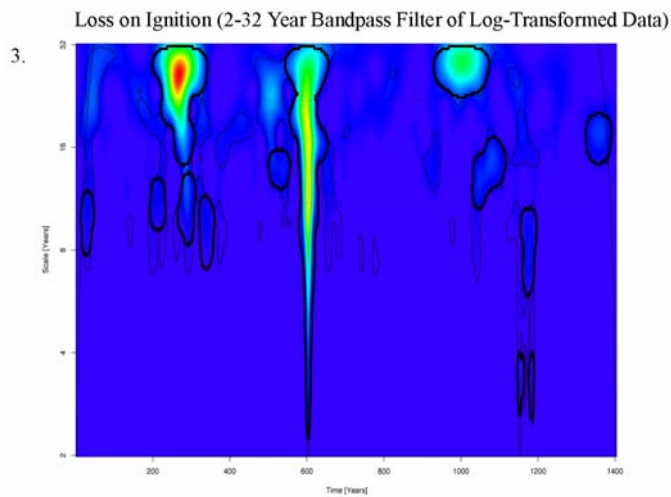
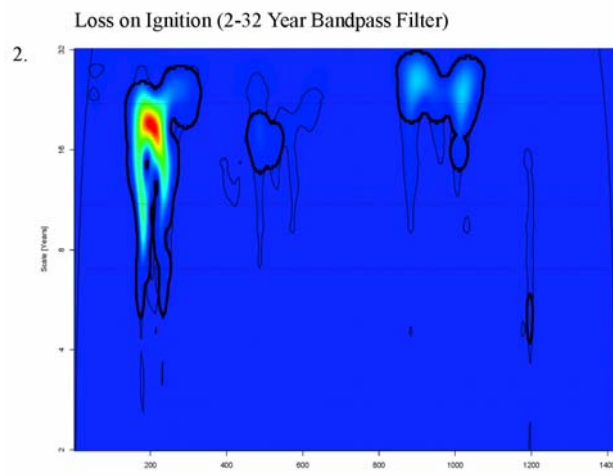
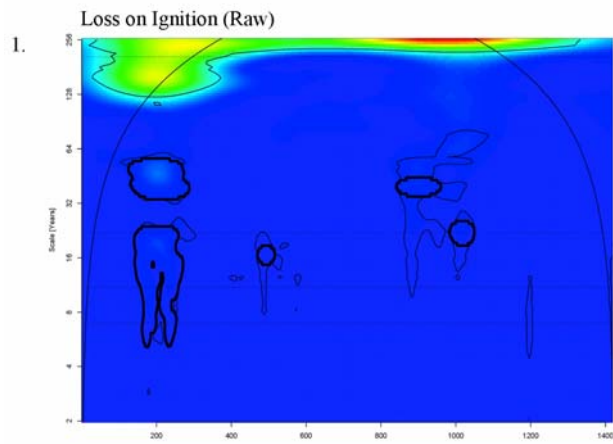


Figure 15: Wavelet power spectra over the time period 1610-1995 A.D. for A) group sunspot number (Hoyt and Schatten, 1998); B) macroscopic charcoal; C) loss on ignition; and D) magnetic susceptibility. Significant wavelet power peaks at the 95% confidence level are delineated by 1) point-wise (thin black lines) and 2) area-wise testing (thick black lines), where the latter significance test is considered more conservative (Maraun and Kurths, 2004).

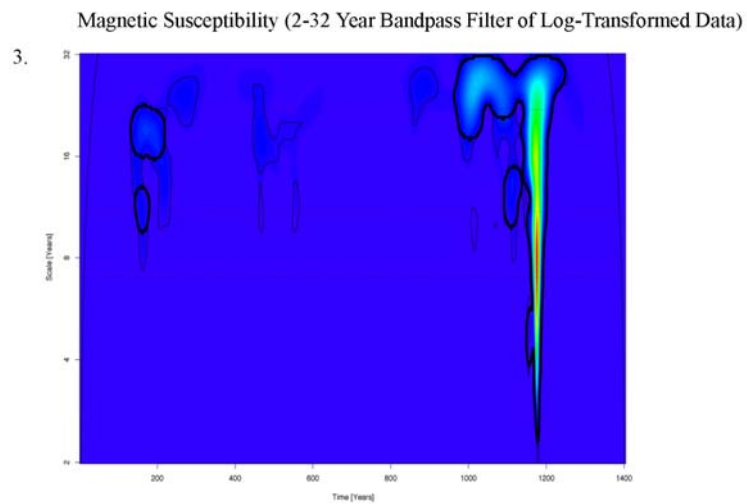
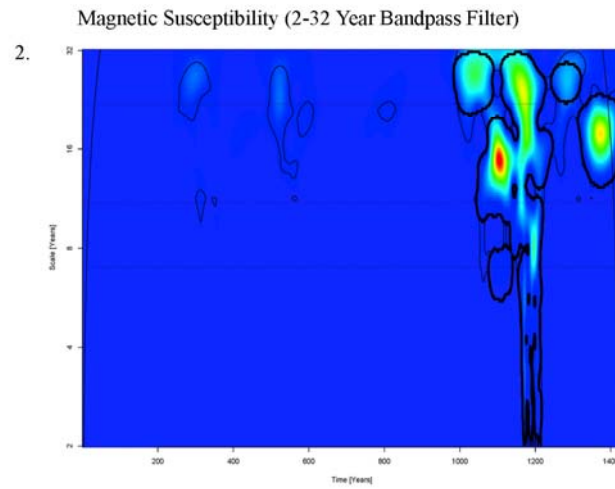
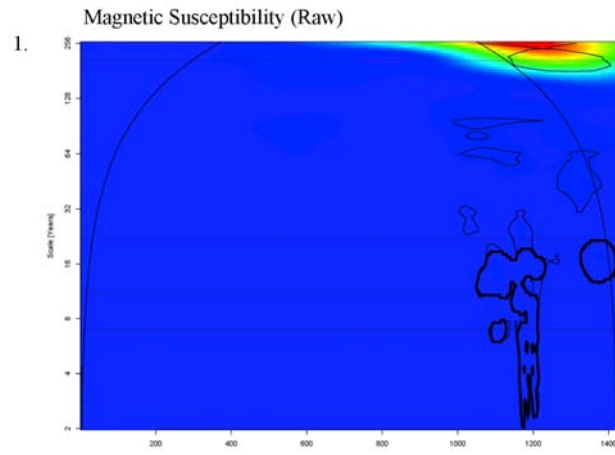
Appendix A1: Macroscopic Charcoal Wavelet Power Spectra



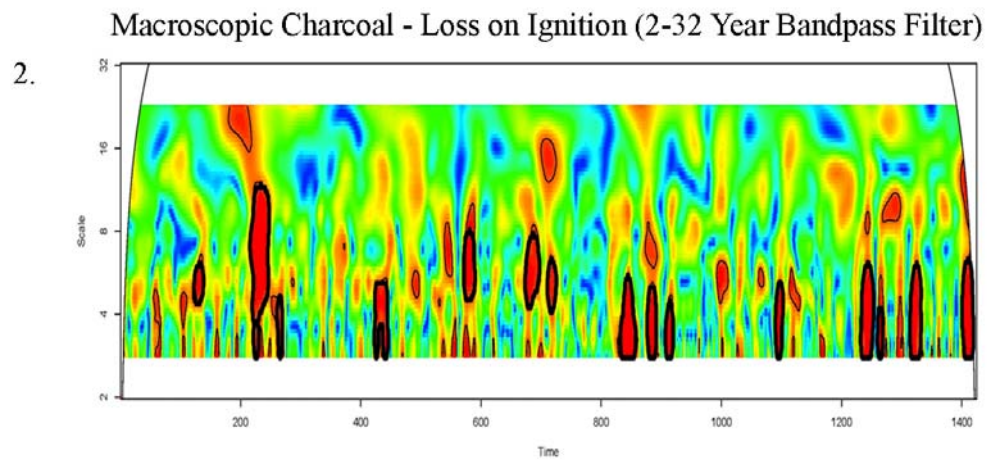
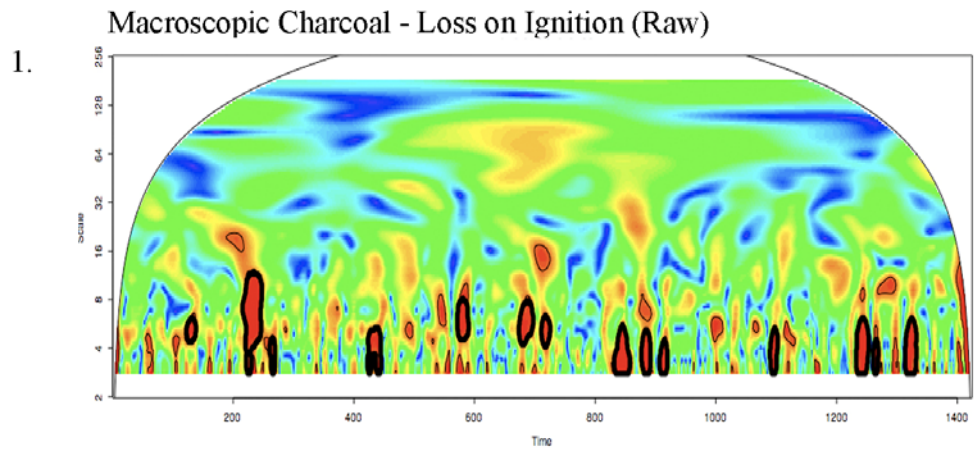
Appendix A2: Loss on Ignition Wavelet Power Spectra



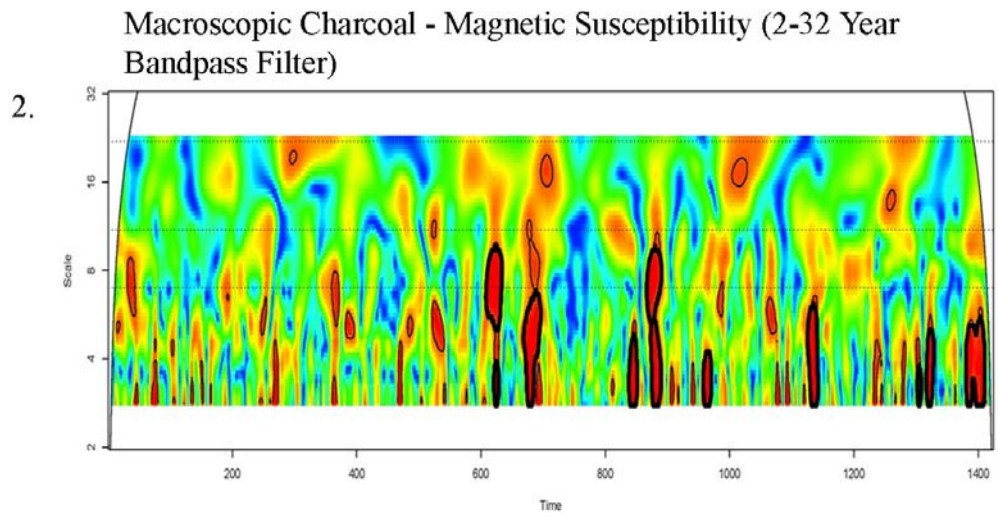
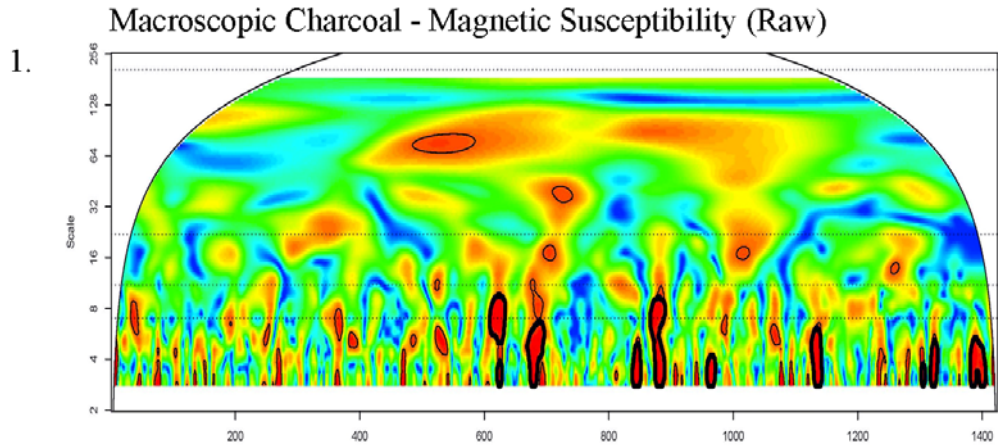
Appendix A3: Magnetic Susceptibility Wavelet Power Spectra



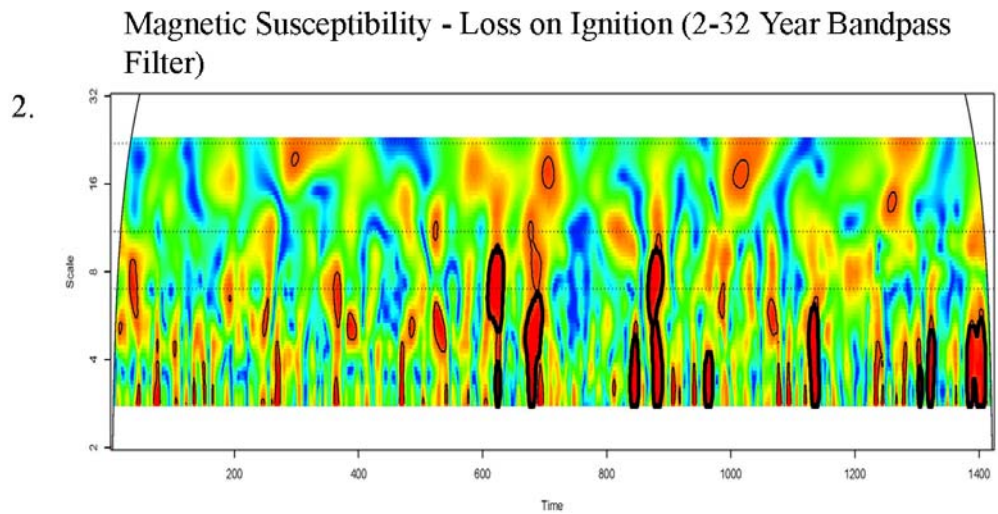
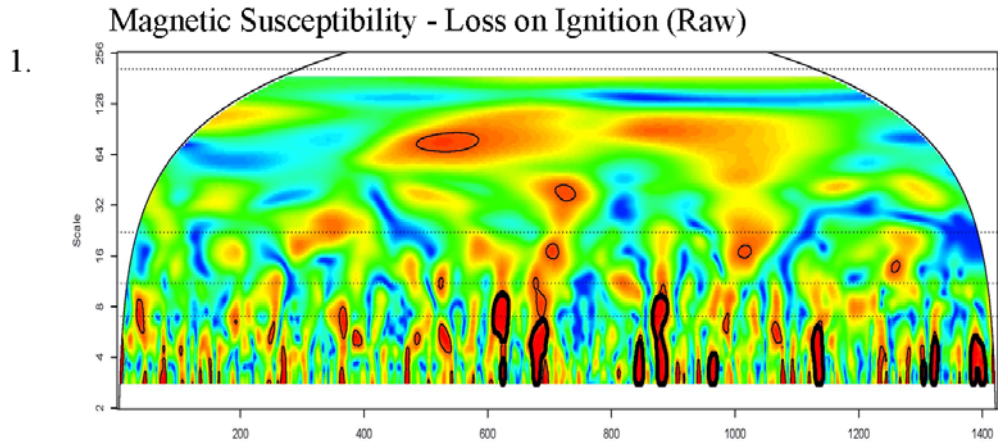
Appendix B1: Macroscopic Charcoal – Loss on Ignition Wavelet Coherency Spectra



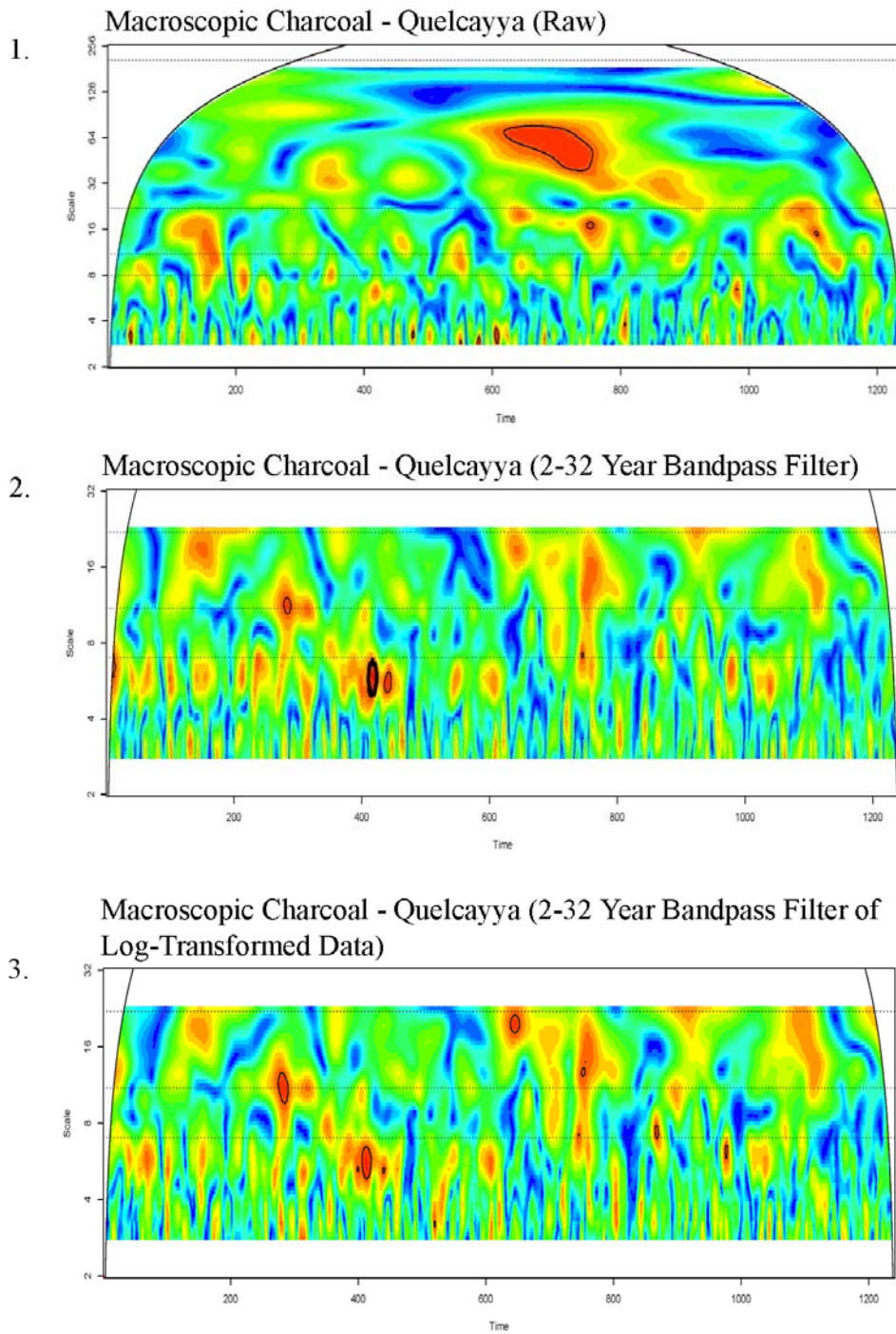
Appendix B2: Macroscopic Charcoal – Magnetic Susceptibility Wavelet Coherency Spectra



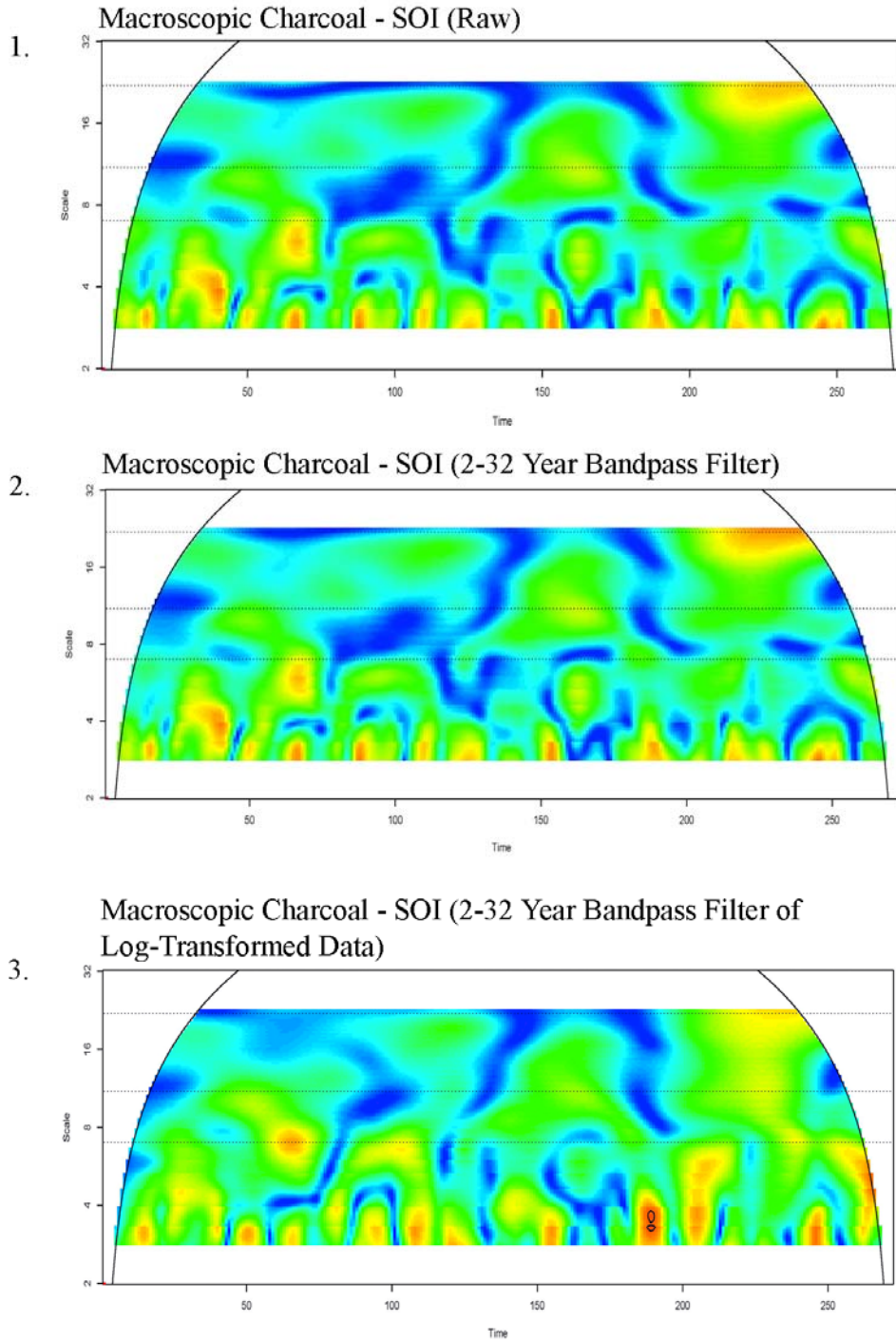
Appendix B3: Magnetic Susceptibility – Loss on Ignition Wavelet Coherency Spectra



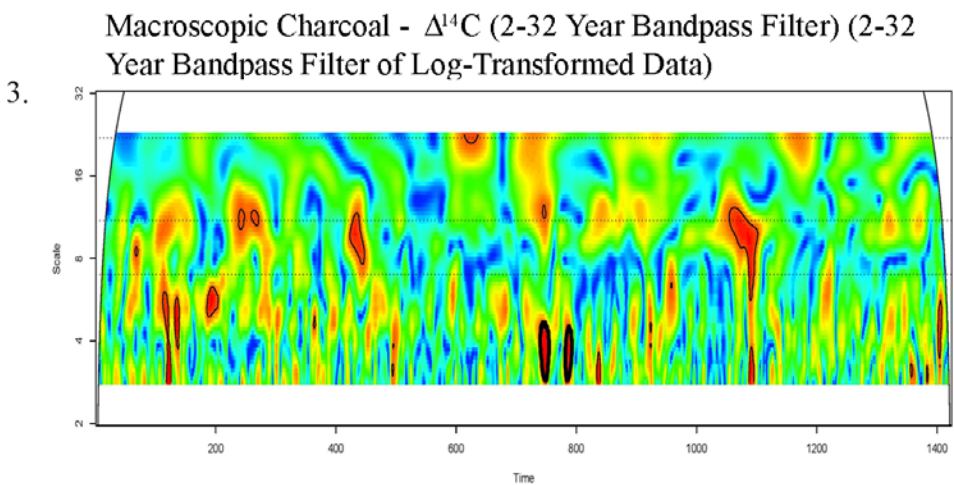
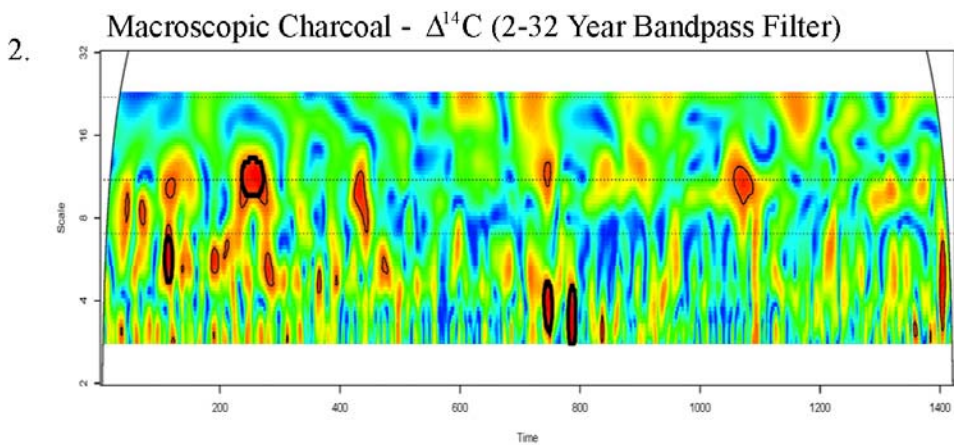
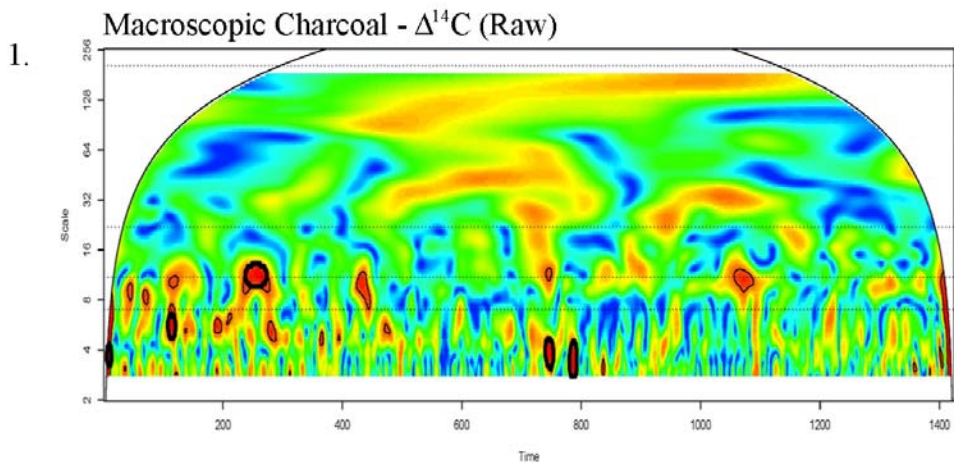
Appendix C1: Macroscopic Charcoal – Quelcayya Snow Accumulation Wavelet Coherency Spectra



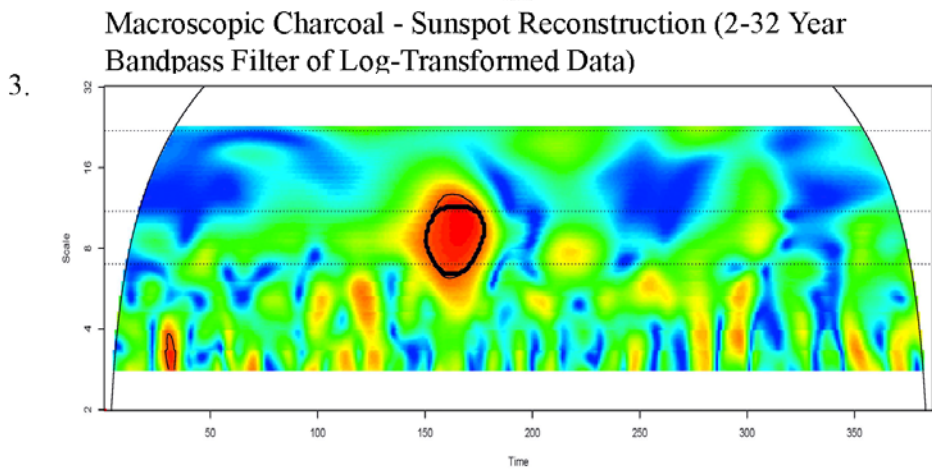
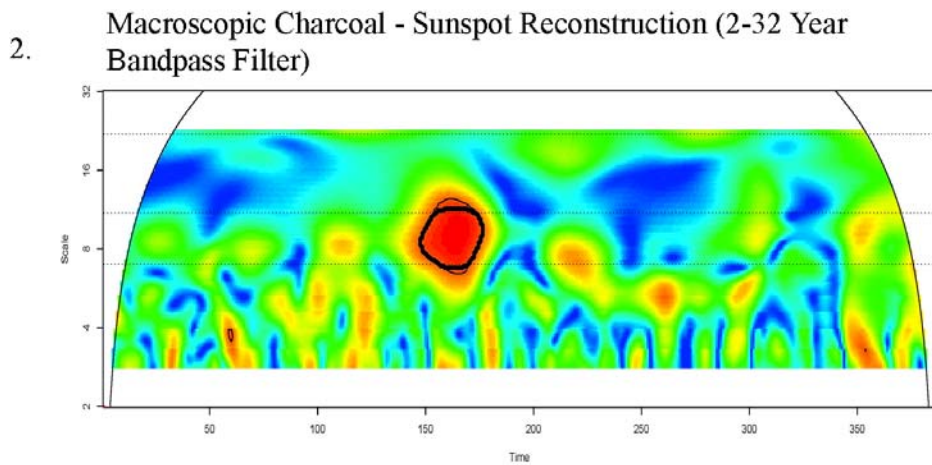
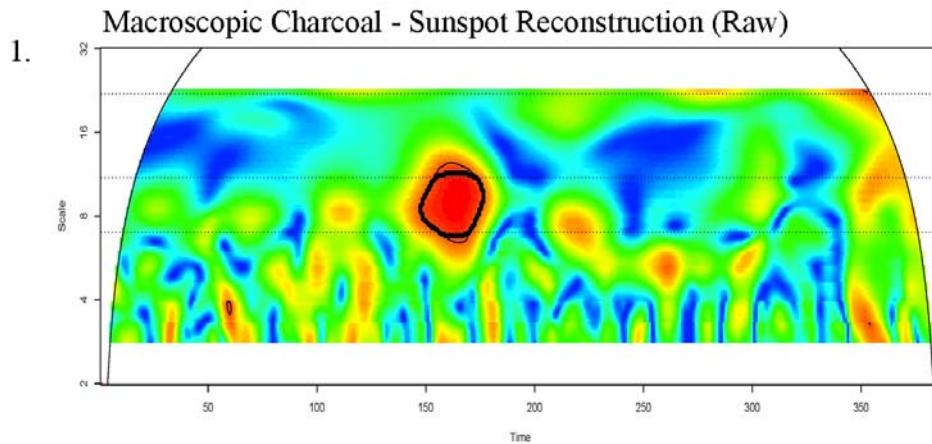
Appendix C2: Macroscopic Charcoal – SOI Wavelet Coherency Spectra



Appendix C3: Macroscopic Charcoal – $\Delta^{14}\text{C}$ Wavelet Coherency Spectra



Appendix C4: Macroscopic Charcoal – Sunspot Reconstruction Wavelet Coherency Spectra



Appendix D – Paleoproxy Data

Depth (cm)	Total Macroscopic Charcoal (Particles/cc)	Charcoal Accumulation Rates (Particles/cc/year)	Loss on Ignition	Magnetic Susceptibility
2	61	-	17	22
4	32	7	17	23
6	52	11	16	19
8	93	20	16	23
10	75	16	16	16
12	38	8	17	13
14	78	17	17	17
16	145	31	16	19
18	38	8	15	16
20	20	4	19	17
22	20	4	20	11
24	20	4	25	13
26	17	4	27	5
28	35	8	24	4
30	43	9	22	5
32	43	9	22	6
34	35	8	23	9
36	17	4	22	9
38	43	9	21	9
40	23	5	21	10
42	6	1	20	13
44	38	8	19	12
46	38	8	18	13
48	14	3	21	15
50	32	7	19	14
52	55	12	19	13
54	26	6	20	12
56	69	15	19	14
58	61	13	20	14
60	12	3	20	14
62	35	8	19	11
64	49	11	19	11
66	17	4	19	8
68	46	10	19	7
70	38	8	27	10
72	29	6	31	10
74	61	13	25	13
76	14	3	34	11

Appendix D – Paleoproxy Data

Depth (cm)	Total Macroscopic Charcoal (Particles/cc)	Charcoal Accumulation Rates (Particles/cc/year)	Loss on Ignition	Magnetic Susceptibility
78	17	4	26	8
80	49	11	38	8
82	67	14	28	6
84	32	7	43	6
86	35	8	40	6
88	32	7	33	8
90	49	11	41	10
92	26	6	58	10
94	23	5	52	6
96	52	11	44	8
98	78	17	37	6
100	6	1	54	9
102	32	7	29	11
104	23	5	23	12
106	9	2	31	23
108	46	10	23	15
110	41	9	28	14
112	17	4	29	15
114	67	14	24	19
116	119	26	18	22
118	55	12	19	17
120	49	11	18	12
122	78	17	18	7
124	14	3	17	12
126	43	9	14	16
128	101	22	16	17
130	12	3	16	9
132	32	7	18	9
134	46	10	14	27
136	17	4	13	22
138	43	9	14	36
140	81	18	16	27
142	43	9	18	19
144	20	4	18	15
146	69	15	17	12
148	55	12	16	18
150	64	14	16	30

Appendix D – Paleoproxy Data

Depth (cm)	Total Macroscopic Charcoal (Particles/cc)	Charcoal Accumulation Rates (Particles/cc/year)	Loss on Ignition	Magnetic Susceptibility
152	78	17	17	20
154	96	21	17	25
156	116	25	18	16
158	124	27	16	24
160	67	14	16	17
162	58	13	16	20
164	49	11	16	20
166	75	16	15	25
168	98	21	18	26
170	136	29	17	20
172	78	17	15	30
174	119	26	18	25
176	87	19	14	26
178	130	28	14	29
180	96	21	16	38
182	81	18	15	31
184	116	25	18	28
186	64	14	14	28
188	55	12	14	28
190	165	36	16	24
192	93	20	16	20
194	98	21	16	21
196	52	11	17	26
198	93	20	17	19
200	156	34	17	18
202	101	22	17	17
204	203	44	18	20
206	177	38	19	22
208	26	6	17	17
210	168	36	11	18
212	109	24	20	21
214	49	11	19	17
216	104	23	17	22
218	100	22	14	27
220	159	34	15	41
222	133	29	14	47
224	130	28	12	40

Appendix D – Paleoproxy Data

Depth (cm)	Total Macroscopic Charcoal (Particles/cc)	Charcoal Accumulation Rates (Particles/cc/year)	Loss on Ignition	Magnetic Susceptibility
226	72	16	14	23
228	75	16	18	20
230	101	22	15	32
232	113	24	14	27
234	26	6	18	21
236	150	33	17	24
238	43	9	17	24
240	156	34	13	22
242	58	13	14	32
244	96	21	14	23
246	127	28	13	20
248	72	16	9	33
250	107	23	14	33
252	67	14	12	37
254	58	13	11	42
256	107	23	12	54
258	139	30	12	53
260	200	43	14	42
262	221	48	16	27
264	243	53	15	23
266	229	50	16	14
268	266	58	18	11
270	292	63	21	0
272	203	44	18	2
274	258	56	17	2
276	197	43	16	2
278	168	36	17	3
280	203	44	20	3
282	260	56	19	3
284	321	70	19	2
286	243	53	19	2
288	232	50	18	3
290	220	48	18	4
292	182	40	18	4
294	203	44	16	9
296	188	41	16	8
298	162	35	16	9

Appendix D – Paleoproxy Data

Depth (cm)	Total Macroscopic Charcoal (Particles/cc)	Charcoal Accumulation Rates (Particles/cc/year)	Loss on Ignition	Magnetic Susceptibility
300	168	36	16	11
302	153	33	17	10
304	165	36	17	13
306	177	38	17	12
308	203	44	17	17
310	194	42	18	15
312	232	50	20	11
314	564	162	19	11
316	506	145	18	14
318	570	164	18	14
320	466	134	19	16
322	446	128	18	18
324	527	151	16	21
326	396	114	15	26
328	414	119	13	33
330	475	136	12	36
332	498	143	13	38
334	530	152	13	29
336	449	129	13	38
338	483	139	13	36
340	420	120	12	39
342	463	133	12	33
344	495	142	13	34
346	463	133	12	33
348	405	116	12	36
350	423	121	12	38
352	732	210	12	41
354	637	183	12	32
356	622	179	12	36
358	614	176	12	28
360	620	178	14	32
362	600	172	13	34
364	559	161	13	42
366	538	154	14	32
368	519	149	15	31
370	504	145	13	33
372	744	108	16	35

Appendix D – Paleoproxy Data

Depth (cm)	Total Macroscopic Charcoal (Particles/cc)	Charcoal Accumulation Rates (Particles/cc/year)	Loss on Ignition	Magnetic Susceptibility
374	587	85	16	37
376	764	111	17	27
378	541	79	16	31
380	640	93	17	29
382	593	86	17	27
384	651	95	18	24
386	700	102	21	24
388	781	114	35	27
390	425	62	24	21
392	255	37	19	22
394	402	59	19	23
396	272	40	23	21
398	420	61	24	22
400	200	29	28	12
402	226	33	32	11
404	388	56	33	9
406	368	53	26	10
408	205	30	26	5
410	145	21	33	6
412	148	21	30	4
414	150	22	30	4
416	243	35	31	5
418	205	30	32	7
420	232	49	31	7
422	220	47	31	8
424	232	49	29	6
426	281	60	32	8
428	165	35	27	14
430	136	29	14	33
432	217	46	10	60
434	200	43	10	68
436	182	39	13	50
438	278	59	8	46
440	188	40	8	44
442	205	44	6	55
444	237	51	8	59
446	119	25	10	54

Appendix D – Paleoproxy Data

Depth (cm)	Total Macroscopic Charcoal (Particles/cc)	Charcoal Accumulation Rates (Particles/cc/year)	Loss on Ignition	Magnetic Susceptibility
448	153	33	11	59
450	269	57	8	30
452	156	33	7	55
454	226	48	7	62
456	237	51	6	62
458	217	46	6	92
460	226	48	5	76
462	179	38	4	80
464	58	12	2	139
466	72	15	1	
468	119	25	1	112
470	122	26	2	168
472	113	24	1	161
474	122	26	2	119
476	90	19	1	153
478	107	23	1	
480	116	25	2	112
482	93	20	1	150
484	72	15	1	137
486	182	39	1	136
488	81	17	1	122
490	148	31	2	149
492	211	45	3	124
494	241	51	3	157
496	279	59	4	173
498	301	288	4	100
500	229	219	4	81
502	182	174	4	145
504	194	185	4	87
506	168	161	3	114
508	171	163	2	97
510	223	213	3	89
512	289	277	3	69
514	240	230	3	103
516	124	119	2	94
518	185	177	3	82
520	356	340	4	81

Appendix D – Paleoproxy Data

Depth (cm)	Total Macroscopic Charcoal (Particles/cc)	Charcoal Accumulation Rates (Particles/cc/year)	Loss on Ignition	Magnetic Susceptibility
522	301	288	5	115
524	260	249	4	89
526	353	338	4	109
528	214	205	4	116
530	321	307	4	113
532	211	202	4	131
534	310	296	4	103
536	341	327	4	78
538	324	310	4	67
540	240	230	4	81
542	266	255	4	109
552	270	258	6	85
554	269	257	6	67
556	388	371	6	74
558	269	257	6	103
560	150	144	5	81
562	156	149	5	126
564	177	169	5	135
566	208	199	5	65
568	205	197	6	82
570	226	216	4	91
572	179	172	6	76
574	275	263	6	85
576	240	230	6	73
578	197	188	6	92
580	460	440	6	
582	200	191	6	89
584	197	188	6	104
586	347	332	5	95
588	263	30	6	75
590	272	31	6	89
592	434	50	5	72
594	379	44	5	
596	359	41	5	51
598	318	37	5	81
600	197	23	4	62
602	156	18	5	

Appendix D – Paleoproxy Data

Depth (cm)	Total Macroscopic Charcoal (Particles/cc)	Charcoal Accumulation Rates (Particles/cc/year)	Loss on Ignition	Magnetic Susceptibility
604	353	41	5	
606	142	16	4	73
608	150	17	4	118
610	373	43	4	157
612	208	24	5	133
614	330	38	6	118
616	605	70	6	95
618	344	40	6	138
620	304	35	6	108
622	573	66	7	145
624	272	31	7	93
626	260	30	7	120
628	420	48	7	81
630	648	75	6	98
632	463	53	7	62
634	582	67	6	53

References

- Agassiz, L. (1840). "Etudes sur les glaciers." Privately published, Neuchatel.
- Alley, R. B., J. Marotzke, W. D. Nordhaus, J. T. Overpeck, D. M. Peteet, R. A. Pielke Jr., R. T. Pierrehumbert, P. B. Rhines, T. F. Stocker, L. D. Talley, and J. M. Wallace (2003). "Abrupt climate change." *Science* 299: 2005-2010.
- Anchukaitis, K.J. and Horn, S.P. (2005). "A 2000-year reconstruction of forest disturbance from southern Pacific Costa Rica." *Palaeogeography, Palaeoclimatology, Palaeoecology* 221: 35-54.
- Barrucand, M., Rusticucci, M., and Vargas, W. (2006). *Proceedings of 8 ICSHMO*. Foz do Iguacu, Brazil, 1491-1499.
- Baudez, C.F. (1970). *Central America*. Geneva: Nagel Publishers.
- Baliunas, S., P. Frick, D. Sokolo, and W. Soon. (1997). "Time scales and trends in the central England temperature data (1659-1990): A wavelet analysis." *Geophysical Research Letters* 24: 1351.
- Behling, H. (2000). "A 2860-Year High-Resolution Pollen and Charcoal Record from the Cordillera de Talamanca in Panama: A History of Human and Volcanic Forest Disturbance." *The Holocene* 10(3): 387-393.
- Bennett, K.D., Boreham, S., Sharp, M.J., and Switsur, V.R. (1992). "Holocene history of environment, vegetation and human settlement on Catta Ness, Lunnasting, Shetland." *Journal of Ecology* 80: 241-273.
- Berglund, B.E. (2003). "Human impact and climate changes - synchronous events and a causal link?" *Quaternary International* 105: 7-12.
- Binford, M. B. and A. L. Kolata (1996). "Climate Variation and the Rise and Fall of an Andean Civilization." *Quaternary Research* 47: 235-248.
- Birks, H.J.B. and Gordon, A.D. (1985). *Numerical Methods in Quaternary Pollen Analysis*. London: Academic Press.
- Bond, G., W. Broecker, J. Sigfus, J. McManus, L. Labeyrie, J. Jouzel, and G. Bonani (1993). "Correlations between climate records from North Atlantic sediments and Greenland ice." *Nature* 365: 143-147.
- Bond, G. and Lotti, R. (1995). "Iceberg discharges into the North Atlantic on millennial time scales during the last deglaciation." *Science* 267: 1005-1010.

- Bond, G., W. Showers, M. Cheseby, R. Lotti, P. Almasi, P. de-Menocal, P. Priore, H. Cullen, I Hafdas, and G. Bonani (1997). "A pervasive millennial-scale cycle in North Atlantic Holocene and glacial climates." *Science* 278: 1257-1266.
- Borgia, A. and B. van Wyk de Vries (2003). "The volcano-tectonic evolution of Concepción, Nicaragua." *Bulletin of Volcanology* 65: 248-266.
- Boyle, E. A. (1987). "North Atlantic thermohaline circulation during the past 20,000 years linked to high-latitude sea surface temperature." *Nature* 330: 35-40.
- Brenner M., Leyden B. and Binford M.W. (1990). "Recent sedimentary histories of shallow lakes in the Guatemalan savannas." *Journal of Paleolimnology* 4: 239–252.
- Brenner M., Leyden B. and Binford M.W. (1990). "Recent sedimentary histories of shallow lakes in the Guatemalan savannas." *Journal of Paleolimnology* 4: 239–252.
- Brenner, M., Rosenmeir, M.F., Hodell, D.A., Curtis, J.H. (2002). "Paleolimnology of the Maya lowlands: long-term perspectives on interactions among climate, environment, and humans." *Ancient Mesoamerica* 13: 141-157.
- Broecker, W. S., G. Bond, and M. Klas (1990). "A salt oscillator in the glacial Atlantic? 1. The concept." *Paleoceanography* 5: 469-477.
- Broecker, W. S., M. Andree, W. Wolfi, H. Oeschger, G. Bonani, J. Kennett, and D. Peteet (1988). "The chronology of the last deglaciation: implications to the cause of the Younger Dryas Event." *Paleoceanography* 3: 1-19.
- Burney, D. A. (1996). "Climate Change and Fire Ecology as Factors in the Quaternary Biogeography of Madagascar." In *Biogeographie de Madagascar*, ed. W. Lourenco: 49-58. Orstom, Paris.
- Bush, M.B. and P.A. Colinvaux. 1994. "Tropical Forest Disturbance: Paleoecological Records from Darien, Panama." *Ecology* 75:1761-1768.
- Carcaillet, C., Bergeron, Y., Richard, P.J.H., Fréchette, B., Gauthier, S., and Prairie, Y.T. (2001). "Change of Fire Frequency in the Eastern Canadian Boreal Forests during the Holocene: Does Vegetation Composition or Climate Trigger the Fire Regime?" *Journal of Ecology* 89(6): 930-946.
- Carmona, R., Hwang, W.L., and Torresani, B. (1998) *Practical Time-Frequency Analysis, Gabor and Wavelet Transforms With an Implementation in S*, San Diego: Academic Press.

- Caviedes, C. N. (1984). "Geography and the Lessons from El Niño." *Professional Geographer* 36: 428–436.
- Caviedes, C. N., and Waylen, P. R. (1993). "Anomalous westerly winds during El Niño events: The discovery and colonization of Easter Island." *Applied Geography* 13(2): 123–134.
- Caviedes, C.N. (2001). *El Niño in History: Storming through the Ages*. Gainesville: University Press of Florida, 2001.
- COHMAP Members (1988). "Climate changes of the last 18,000 years: Observations and model simulations." *Science* 241: 1043-1052.
- Clement, R.M, and S.P. Horn. 2001. "Pre-Columbian Land-Use History in Costa Rica: A 3000-Year Record of Forest Clearance, Agriculture and Fires From Laguna Zoncho." *The Holocene* 11(4): 419-426.
- Cochrane, M. A., Alencar, A., Schulze, M. D., Souza, C. M. J., Nepstad, D. C., Lefebvre, P., and Davidson, E. A. (1999). "Positive feedbacks in the fire dynamic of closed canopy tropical forests." *Science* 284, 1832-1835.
- Cullen, H.M., deMenocal, P.B., Hemming, S., Hemming, G., Brown, F.H., Guilderson, T. and Sirocko, F. (2000). "Climate change and the collapse of the Akkadian Empire; evidence from the deep sea." *Geology* 28: 379-382.
- Crutzen, P. J., and E. F. Stoermer (2000) "The 'Anthropocene'." *Global Change Newsletter* 41: 12-13.
- Dansgaard, W., Johnsen, S., Clausen, H., Dahl-Jensen, D., Gundestrup, N., Hammer, C., Hvidbeg, C., Steffensen, J., Sveinbjornsdottir, A., Jouzel, J. and Bond, G. (1993). "Evidence for a general instability of the past climate from a 250 kyr ice core record." *Nature* 364: 218-220.
- Dean, W.E. Jr., (1974). "Determination of carbonate and organic matter in calcareous sediments and sedimentary rocks by loss on ignition: Comparison with other methods." *Journal of Sedimentary Petrology* 44: 242–248.
- Dean, J.S., Euler, R.C., Gumerman, G.J., Plog, F., Hevly, R.H., and Karlstrom, T.N.V. (1985) "Human Behavior, Demography, and Paleoenvironment on the Colorado Plateaus." *American Antiquity* 50: 537-554.
- Dearing, J. (1999). *Operation manual, Bartington Instruments Ltd. Environmental magnetic susceptibility – Using the Bartington MS2 system*. London: Chi Publishing.

- DeBano, L.F., Neary, D.G., P.F. Folliot (1998). *Fire's Effects on Ecosystems*. New York, New York: John Wiley & Sons, Inc.
- Demarest, A.A., Rice, P.M., Rice, D.S. (2004). "The Terminal Classic in the Maya lowlands: assessing collapses, terminations, and transformations." In *The Terminal Classic in the Maya Lowlands: Collapse, Transition, and Transformation*, Demarest, A.A., Rice, P.M., Rice, D.S. (Eds.), Boulder: University of Colorado Press, 545-572.
- DeMenocal, P.B. (2001). "Cultural responses to climate change during the late Holocene." *Science* 292: 667-673.
- Denevan, W. M. (1961). "The upland pine forests of Nicaragua." *University of California Publications in Geography* 12: 251-320.
- Denevan, W. M. (1992). "The Pristine Myth: The Landscape of the Americas in 1492." *Annals of the Association of American Geographers* 82: 369-385.
- Denton, G. H., and Karlen, W. (1973). "Holocene climatic variations—their pattern and possible cause." *Quaternary Research* 3: 155-205.
- Diaz, H. F., and Markgraf, V. (1992). *El Niño: Historical and Paleoclimatic Aspects of the Southern Oscillation*. Cambridge University Press, 476 pp.
- Doolittle, B. (2000). *Cultivated Landscapes of Native North America*. Oxford: Oxford University Press.
- Dull, R. (2004a). "An 8000-year record of vegetation, climate, and human disturbance from the Sierra de Apaneca, El Salvador." *Quaternary Research* 61(2): 159-167.
- Dull, R. (2004b). "A Holocene record of Neotropical savanna dynamics from El Salvador." *Journal of Paleolimnology* 32: 219-231.
- Enquist, B. J., and Leffler, A. J. (2001). "Long-term tree ring chronologies from sympatric tropical dry-forest trees: individualistic responses to climatic variation." *Journal of Tropical Ecology* 17, 41-60.
- Faegri, K. and J. Iversen. (1989). *Textbook of Pollen Analysis*. John Wiley & Sons: New York, 328 p.
- Fagan, B. (1999). *Floods, Famines and Emperors: El Niño and the Fate of Civilizations*, New York: Basic Books.

- Farge, M. (1992). "Wavelet transforms and their applications to turbulence." *Annual Review of Fluid Mechanics* 24: 395-457.
- Fligge, M., S.K. Solanki, and J. Beer. (1999). "Determination of solar cycle length variations using the continuous wavelet transform." *Astrophysics* 346: 313-321.
- Gamage, N., and Blumen, W. (1993). "Comparative analysis of low-level cold fronts: Wavelet, Fourier, and empirical orthogonal function decompositions." *Monthly Weather Review* 121: 2867-2878.
- Gill, R.B. (2000). *The Great Maya Droughts: Water, Life, and Death*. Albuquerque: University of New Mexico Press.
- Glantz, M. H. (1987). *The Societal Impacts Associated with the 1982–83 Worldwide Climate Anomalies*, National Center for Atmospheric Research, Boulder.
- Glantz, M. H. (1994). *Usable Science: Food Security, Early Warning, and El Niño*, National Center for Atmospheric Research, Boulder.
- Glantz, M. H. (2001). "Currents of change: impacts of El Niño and La Niña on climate and society." Cambridge University Press, Cambridge.
- Grinsted, A., Moore J.C., and S. Jevrejeva. (2004). "Application of the cross wavelet transform and wavelet coherence to geophysical time series." *Nonlinear Processes in Geophysics* 11: 561-566.
- Haberland, W. 1986. "Settlement Patterns and Cultural History of Ometepe Island, Nicaragua: A Preliminary Sketch." *Journal of the Steward Anthropological Society* 14: 369-386.
- Haberle, S.G. (1996). "Palaeoenvironmental changes in the eastern highlands of Papua New Guinea." *Archaeology in Oceania* 31(1): 1-11.
- Haberle, S.G. (1998a). "Late Quaternary vegetation change in the Tari Basin, Papua New Guinea." *Palaeogeography, Palaeoclimatology, Palaeoecology* 137: 1-24.
- Haberle, S.G. (1998b). "Dating the evidence for prehistoric agricultural change in the highlands of New Guinea: the last 2000 years." *Australian Archaeology* 47: 1-19.
- Haberle, S.G. (2001). "Vegetation response to climate variability: a palaeoecological perspective on the ENSO phenomenon." In *El Niño: History and Crisis*. Eds. R. Grove and J. Chappell. The White Horse Press: Cambridge, England, pps. 66-78.

- Haberle, S.G., Ledru, M.-P. (2001). "Correlations among charcoal records of fires from the past 16000 years in Indonesia, Papua-New Guinea and Central and South America." *Quaternary Research* 55: 97–104.
- Haberle, S.G. and David, B. (2004). "Climates of change: human dimensions of Holocene environmental change in low latitudes of the PEPH transect." *Quaternary International* 118-119: 165-179.
- Haug, G.H., Gunther, D., Peterson, L.C., Sigman, D.M., Hughen, K.A. and Aeschlimann, B. (2003). "Climate and the collapse of Maya civilization." *Science* 299: 1731-1735.
- Heiri, O., A. F. Lotter, and G. Lemcke. (2001). "Loss on ignition as a method for estimating organic and carbonate content in sediments: Reproducibility and comparability of results." *Journal of Paleolimnology* 25: 101-110.
- Hewitt, K. (1983). *Interpretations of Calamity from the Viewpoint of Human Ecology*, London: Allen & Unwin.
- Hoffman, M. P. (1980). "Prehistoric ecological crises." In *Historical Ecology: Essays on Environment and Social Change*, Bilsky, L. J. (ed.), New York: Kennikat Press, 33–41.
- Hodell, DA, Curtis, JH and Brenner, M. (1995). "Possible role of climate in the collapse of the Classic Maya Civilization." *Nature* 375: 391-394.
- Hodell, D.A., Brenner, M. and Curtis, J.H. (2005). "Terminal Classic drought in the northern Maya lowlands inferred from multiple sediment cores in Lake Chichancanab (Mexico)." *Quaternary Science Reviews* 24: 1413-1427.
- Hodell, D.A., Brenner, M., Curtis, J.H. and Guilderson, T. (2001). "Solar forcing of drought frequency in the Maya lowlands." *Science* 292: 1367-1369.
- Horn, S.P. (1993). "Postglacial vegetation and fire history in the Chirripó Páramo of Costa Rica." *Quaternary Research* 40: 107–116.
- Horn, S. P. & R. L. Sanford. (1992). "Holocene fires in Costa Rica." *Biotropica* 24(3): 354-361.
- Hoyt, D.V. and Schatten, K.H. (1998). "Group Sunspot Numbers: A new Solar Activity Reconstruction." *Solar Physics* 181: 491-512.
- Heusser, C.J. (1971). *Pollen and spores of Chile*. University of Arizona Press: Tucson, 167 p.

- Ihaka, R. and R. Gentleman. (1996). "R: A Language for Data Analysis and Graphics." *Journal of Computational and Graphical Statistics* 5: 299-314.
- Ikuse, M. (1956). *Pollen Grains of Japan*. Hirokawa Publishing Co.: Tokyo.
- Imbrie, J., and Imbrie, J.Z. (1980). "Modeling the climatic response to orbital variations." *Science* 207: 943-953.
- International Institute of Environment and Development/World Resources Institute. (1987). *World Resources 1987*. New York: Basic Books.
- Janzen, D. H. (1988). "Tropical dry forest: the most endangered major tropical ecosystem." In *Biodiversity*. E. O. Wilson, and F. M. Petere, Eds. pp. 130-137. National Academy Press, Washington, D.C.
- Jevrejeva, S., Moore, J.C., and A. Grinsted, (2003). "Influence of the Arctic Oscillation and El Niño-Southern Oscillation (ENSO) on ice conditions in the Baltic Sea: The wavelet approach." *Journal of Geophysical Research* 108: 4677-4687.
- Johnson, N. C., and Wedin, D. A. (1997). "Soil, carbon, nutrients, and mycorrhizae during conversion of dry tropical forest to grassland." *Ecological Applications* 7, 171-182.
- Kauffman, J. B., Sanford, R. L., Cummings, D. L., Salcedo, I. H., and Sampaio, E. V. S. B. (1993). "Biomass and nutrient dynamics associated with slash fires in Neotropical dry forests." *Ecology* 74: 140-151.
- Kellman, M., and J. Meave (1997). "Fire in the tropical gallery forests of Belize." *Journal of Biogeography* 24: 23-34.
- Keitt, T. H. and D. L. Urban. (2005). "Scale-specific inference using wavelets." *Ecology* 86: 2497-2504.
- Keitt, T. H. and J. Fischer. (2006). "Detection of scale-specific community dynamics using wavelets." *Ecology* 87: 2895-2904.
- Koonce, A. L. and Caban-Gonzalez, A. (1990). Social and ecological aspects of fire in Central America. In: *Fire in the Tropical Biota*. J.G. Goldammer (Ed.). Springer-Verlag: Berlin, Germany. pp. 135-158.
- Knapp, R.O., Davis, O.K., and King, J.E. (2000). *Guide to Pollen and Spores*. W.C. Brown Co. Publishing: Dubuque, Iowa, 279 p.
- Kumar, P. and Foufoula-Georgiou, E. "Wavelet analysis for geophysical applications." *Reviews of Geophysics* 35(4): 385-412.

- Lamprecht, H. 1989. Silviculture in the Tropics. *Tropical forest ecosystems and their tree species; possibilities and methods for their long-term utilization*. Deutsche Ges. f. techn. Zusammenarbeit (GTZ), Eschborn.
- Lange, F.W. (1984). "The Greater Nicoya Archaeological Subarea," In *The Archaeology of Lower Central America*. Eds. Lange, F. and Stone, D., Albuquerque: University of Mexico Press, pp. 165-194.
- Lange, F.W., P.D. Sheets, A. Martinez, and S. Abel-Vidor. (1992). *The Archaeology of Pacific Nicaragua*. Albuquerque: University of New Mexico Press.
- Lau, K.M. and Weng, H.Y. (1995). "Climate signal detection using wavelet transform: How to make a time series sing." *Bulletin of the American Meteorological Society* 76: 2391-2402.
- Laurance, W. F., and Williamson, B. (2001). "Positive feedbacks among forest fragmentation, drought, and climate change in the Amazon." *Conservation Biology* 15: 1529-1535.
- League, B. and Horn, S. (2000). "A 10,000 year record of Paramo fires in Costa Rica." *Journal of Tropical Ecology* 16: 747-752.
- Levine, J.S. (Ed.) 1985. *The Photochemistry of Atmospheres: Earth, the Other Planets, and Comets*. Academic Press, Sand Diego, California, 500 pages.
- Levine, J.S. (Ed.). 1991. *Biomass Burning: Atmospheric, Climatic, and Biospheric Implications*. The MIT Press, Cambridge, Massachusetts, 569 pages.
- Levine, J. S., W. R. Cofer, D. R. Cahoon, and E. L. Winstead. (1995). "Biomass Burning: A Driver for Global Change." *Environmental Science and Technology* 29: 120A-125A.
- Lewis, H.T. (1973). *Patterns of Indian Burning in California: Ecology and Ethnohistory*, ed. Lowell John Bean. Ballena Anthropological Papers Vol. 1. Ramona, CA: Ballena Press.
- Leyden, B.W., M. Brenner, and B.H. Dahlin. (1998). "Cultural and Climatic History of Coba, a Lowland Maya City in Quintana Roo, Mexico." *Quaternary Research* 49: 111-122.
- Lyell, C. (1830–1833). *Principles of Geology*, 3 vols., Murray, London. Reprinted 1990, University of Chicago Press, Chicago.

- MacDonald, G. M., Larson, C. P. S., Szeicz, J. M., and Moser, K. A. (1991). "The reconstruction of boreal forest fire history from lake sediments: a comparison of charcoal, pollen, sedimentological, and geochemical indices." *Quaternary Science Reviews* 10: 53-71.
- Mallat, S. A. (1998). *Wavelet Tour of Signal Processing*, Sand Diego: Academic Press.
- Messenger, L.C. Jr. (2002). "Los Mayas y El Niño: Paleoclimatic correlations, environmental dynamics, and cultural implications for the ancient Maya." *Ancient Mesoamerica* 13: 159-170.
- Meyer, G. A., Wells, S. G., Balling, R. C., Jr., and Jull, A. J. T. (1992). "Response of alluvial systems to fire and climate change in Yellowstone National Park." *Nature* 357: 147-150.
- Milankovitch, M. (1938). "Astronomische Mittel zur Erforschung der erdgeschichtlichen Klimate." *Handbuch der Geophysik* 9: 593-698.
- Moore, P.D. Webb, J.A., and Collinson, M.E. (1991). *Pollen analysis*. Blackwell Scientific: London, 216 p.
- Moussas, X., Polygiannakis, J.M., Preka-Papadema, P., and G. Exarhos (2005). "Solar cycles: A tutorial." *Advances in Space Research* 35: 725-738.
- Mullings, C. E. (1977). "Magnetic susceptibility of the soil and its significance in Soil Science: a review." *Journal of Soil Science* 28: 223-246.
- Murphy, P. G., and Lugo, A. E. (1986). "Ecology of tropical dry forest." *Annual Review of Ecology and Systematics* 17, 67-88.
- National Research Council Committee Members. (1999). *Human Dimensions of Global Environmental Change: Research Pathways for the Next Decade*. Washington, D.C.: National Academy Press.
- Neff, H. Pearsall D.M, Jones, J.G. Arroyo de Pieters, B., and Freidel, D.E. (2005). "Climate change and population history in the Pacific Lowlands of Southern Mesoamerica." *Quaternary Research*, in press.
- Nepstad, D. C., Verisso, A., Alencar, A., Nobre, C., Lima, E., Lefebvre, P., Schlesinger, P., Potter, C., Moutinho, P., Mendoza, E., Cochrane, M., and Brooks, V. B. (1999). "Large-scale impoverishment of Amazonian forest by logging and fire." *Nature* 398, 505-508.
- Norweb, A.H. (1964). "Ceramic Stratigraphy in Southwestern Nicaragua." In *Actas, 35th International Congress of Americanists* 1: 551-561.

- Ortloff, C.R. and A.L. Kolata. (1993). "Climate and response: agro-ecological perspectives on the decline of the Tiwanaku State." *Journal of Archaeological Science* 20:195-221.
- Otterstrom, S.M. (2002). "Anthropogenic Fire Disturbance in the Tropical Dry Forest of Nicaragua." In *Conference Abstracts, Association for Tropical Biology Annual Meeting*. STRI. Panama City, Panamá. July 29-August 3, 2000.
- Parker, F.D. (1964). *The Central American Republics*. London: Oxford University Press.
- Pierce, J.L., Meyer, G.A. and Jull, A.J.T. (2004). "Fire-induced erosion and millennial-scale climate change in northern ponderosa pine forests." *Nature* 432: 87-90.
- Pyne, S.J. (1998). "Forged in fire: history, land, and anthropogenic fire." In *Advances in Historical Ecology*. Ed. William Balee. Columbia University Press.
- Reimer, PJ, Baillie, MGL, Bard, E, Bayliss, A, Beck, JW, Blackwell, PG, Buck, CE, Burr, GS, Cutler, KB, Damon, PE, Edwards, RL, Fairbanks, RG, Friedrich, M, Guilderson, TP, Herring, C, Hughen, KA, Kromer, B, McCormac, FG, Manning, SW, Ramsey, CB, Reimer, PJ, Reimer, RW, Remmele, S, Southon, JR, Stuiver, M, Talamo, S, Taylor, FW, van der Plicht, J, and Weyhenmeyer, CE. (2004). "IntCal04 Terrestrial radiocarbon age calibration, 0-26 cal kyr BP." *Radiocarbon* 46(3): 1029-1058.
- Rind, D. (2002). "The sun's role in climate variations." *Science* 296: 673-677.
- Roberts, S.J. (2000). "Tropical fire ecology." *Progress in Physical Geography* 24: 281-288.
- Rollins, H. B., Sandweiss, D. H., and Richardson, J. B., III (1986). "The birth of El Niño: Geoarchaeological evidence and implications." *Geoarchaeology* 1: 3-15.
- Ruddiman, W. F. and Thomson, J. S. (2001). "The Case for Human Causes of Increased Atmospheric CH₄ over the Last 5000 Years." *Quaternary Science Reviews* 20: 1769-1779.
- Saarnak, C. F. (2001). "A shift from natural to human-driven fire regime: implications for trace-gas emissions." *Holocene* 11: 373-375.
- Sabogal, C. (1992). "Regeneration of tropical dry forests in Central America, with examples from Nicaragua." *Journal of Vegetation Science* 3: 407-416.
- Sale, K. (1990). *The conquest of paradise: Christopher Columbus and the Columbian legacy*. New York, NY: Alfred A. Knopf

- Sampaio, E. V. S. B., Salcedo, I. H., and Kauffman, J. B. (1993). "Effect of different fire severities on coppicing of caatinga vegetation in Serra Talhada, PE, Brazil." *Biotropica* 25, 452-460.
- Sandgren, P. & Snowball, I.F. (2001). "Application of mineral magnetic techniques to paleolimnology." In *Tracking Environmental Changes in Lake Sediments: Physical and Chemical Techniques. Developments in Paleoenvironmental Research Book Series*, W.M. Last & J.P. Smol (eds.), Kluwer Academic Publishers, 217-237.
- Sandweiss, D. H. (1986). "The beach ridges at Santa, Peru: El Niño, uplift, and prehistory." *Geoarchaeology* 1: 17–28.
- Sandweiss, D. H., Richardson, J. B., III, Reitz, E. J., Rollins, H. B., and Maasch, K. A. (1996). "Geoarchaeological evidence from Peru for a 5000 years B.P. onset of El Niño." *Science* 273: 1531–1533.
- Sanford, Jr., R. L., J. Saldarriaga, K. Clark, C. Uhl, and R. Herrera. (1985). "Amazon rain-forest fires." *Science* 227: 53-55.
- Sauer, C.O. (1956). "The Agency of Man on the Earth." In *Man's Role in Changing the Face of the Earth*, ed. Williams L. Thomas, 49-69. Chicago: University of Chicago Press.
- Scott, G.A.J. (1977). "The role of fire in the creation and maintenance of savanna in the Montaña of Peru." *Journal of Biogeography* 4: 143-167.
- Schimmelmann, Lange, C. B., and Meggers B. J. (2003). "Palaeoclimatic and archaeological evidence for a 200-yr recurrence of floods and droughts linking California, Mesoamerica and South America over the past 2000 years." *The Holocene* 13: 763-778.
- Sheets, P. (1979). "Environmental and cultural effects of the Ilopango eruption in central America." In *Volcanic Activity and Human Ecology*, Sheets, P., and Grayson, D. (eds.), New York: Academic Press, 525–564.
- Sheets, P. (1999). "The effects of explosive volcanism on ancient egalitarian, ranked, and stratified societies in middle America. In *The Angry Earth: Disaster in Anthropological Perspective*, Oliver-Smith, A., and Hoffman, S. M. (eds.), Routledge, New York and London, 36–58.
- Shimada, I, Schaaf, C.B., Thompson, L.G., and Moseley-Thompson, E. (1991). "Cultural impacts of severe drought in the prehistoric Andes." *World Archaeology* 22: 247-270.

- Siegert, F. and Hoffmann, A.A. (2000). "The 1998 forest fires in East Kalimantan (Indonesia): a quantitative evaluation using high resolution, multitemporal ERS-2 SAR images and NOAA-AVHRR hotspot data." *Remote Sensing of the Environment* 72:64-77.
- Sluyter, A. (1997). "Regional, Holocene records of the human dimension of global change: sea-level and land-use change in prehistoric Mexico." *Global and Planetary Change* 14: 127-146.
- Stahle, D.W., R.D. D'Arrigo, P.J. Krusic, M.K. Cleaveland, E.R. Cook, R.J. Allan, J.E. Cole, R.B. Dunbar, M.D. Therrell, D.A. Gay, M.D. Moore, M.A. Stokes, B.T. Burns, J. Villanueva-Diaz and L.G. Thompson. (1998). "Experimental dendroclimatic reconstruction of the Southern Oscillation." *Bulletin of the American Meteorological Society* 79: 2137-2152.
- Stewart, O. (1956). "Fire as the First Great Force Employed by Man." In *Man's Role in Changing the Face of the Earth*, ed. Williams L. Thomas. Chicago: University of Chicago Press, 115-133.
- Stone, D.S. (1977). *Pre-Columbian Man Finds Costa Rica*. Cambridge: Peabody Museum Press.
- Stuiver, M., Reimer, P.J., Bard, E., Beck, J.W., Burr, G.S., Hughen, K.A., Kromer, B., McCormac, G., van der Plicht, J., Spurk, M. (1998). "INTCAL98 radiocarbon age calibration, 24,000–0 cal BP." *Radiocarbon* 40: 1041–1083.
- Stuiver, M., P.M. Grootes, and T.F. Braziunas (1995). "The GISP2 ^{18}O climate record of the past 16,500 years and the role of the sun, ocean and volcanoes." *Quaternary Research* 44: 341-354.
- Suman, D.O. (1991). "A Five Century Sedimentary Geochronology of Biomass Burning in Nicaragua and Central America." In *Global Biomass Burning: Atmospheric, Climatic, & Biospheric Implications*, ed. J.S. Levine, Cambridge: MIT Press, 512-518.
- Thompson, L. G., E. Mosley-Thompson, J. F. Bolzan and B. R. Koci. (1985). "A 1500 year record of tropical precipitation recorded in ice cores from the Quelccaya Ice Cap, Peru." *Science* 229(4717): 971-973.
- Thompson, L.G., E. Mosley-Thompson and Benjamin Morales Arnao. (1984). "Major El Niño/Southern Oscillation events recorded in stratigraphy of the tropical Quelccaya Ice Cap." *Science* 226 (4670): 50-52.

- Torrence, C., and Compo, G.P. (1998). "A practical guide to wavelet analysis." *Bulletin of the American Meteorological Society* 79: 61–78.
- Tsukada, M. and E.S. Deevey. (1967). "Pollen analyses from four lakes in the southern Maya area of Guatemala and El Salvador." In *Quaternary Paleoecology*, E. J. Cushing and H.E. Wright (Eds.), New Haven: Yale University Press, 303-331.
- Urban, F.E., Cole, J.E., and Overpeck, J.T. (2000). "Influence of Mean Climate Change on Climate Variability from a 155-year Tropical Pacific Coral Record." *Nature* 407: 989-993.
- Urquhart, G. R. 1999. "Paleoecological persistence of *Raphia taedigera* swamps in Nicaragua." *Biotropica* 31: 565-569.
- Urquhart, G. R. 1997a. "Paleoecological evidence of *Raphia* in the pre-Columbian Neotropics." *Journal of Tropical Ecology* 13: 793-802.
- Urquhart, G. R. 1997b. Paleoecology of the Laguna Negra swamp near Bluefields, Nicaragua. *Tierra* 2(3): 14-16.
- Vale, Thomas. (2002). "The pre-European landscape of the United States." In *Fire, Native Peoples, and the Natural Landscape*. Ed. Thomas R. Vale. Washington, D.C.: Island Press, 1-39.
- Van Buren, M. (2001). "The archaeology of El Niño Events and Other 'Natural' Disasters." *Journal of Archaeological Method and Theory* 8(2): 129-149.
- Van der Werf, G.R., Randerson, J.T., Collatz, G.J., Giglio, L., Kasibhatla, P.S., Arellano Jr., A.F., Olsen, S.C., Kasischke, E.S. (2004). "Continental-scale partitioning of fire emissions during the 1997 to 2001 El Niño/La Niña period." *Science* 303: 73-76.
- Van West, C. R. 1991. "Reconstructing prehistoric climatic variability and agricultural production in southwestern Colorado, A.D. 901-1300: A GIS approach." In *Proceedings of the Anasazi Symposium 1991*. Eds. Hutchinson, A., Smith, J. E. and Usher, J. Mesa Verde, CO: Mesa Verde Museum Association, Inc., 25-34.
- Van Wyk de Vries, B. and O. Merle (1996). "The effect of volcanic constructs on rift fault patterns." *Geology* 24(7): 643-646.
- Von Post, L. (1946). "The Prospect for Pollen Analysis in the Study of the Earth's Climatic History." *New Phytologist* 45: 198-203.
- Whitlock, C. and C. Larsen. (2001). "Charcoal as a fire proxy." In *Tracking Environmental Change Using Lake Sediments. Volume 3: Terrestrial, Algal, and*

Siliceous Indicators. J.P. Smol , H.J.B. Birks and W.M. Last, eds., Dordrecht: Kluwer Academic Publishers.

Weng, H.Y. and Lau, K.M. (1994). "Wavelet, period-doubling and time-frequency localization with application to satellite data analysis." *Journal of Atmospheric Science* 51: 2523-2541.

Wiley, G.R. *An Introduction to American Archeology, vol. 1, North and Middle America*. Englewood Cliffs, N.J.: Prentice-Hall.

The vita has been removed from the reformatted version of this document.